E-BEAM HCl LASER

John A. Shirley, et al

United Aircraft Research Laboratories

Prepared for:

Office of Naval Research
Advanced Research Projects Agency

30 August 1974

AD 784 500

Security Classification

DOCUMENT CONTROL DATA · R & D

Security classification of title, body of abstract and indexing annotation must be entered when the overall report is classified)

1. ORIGINATING ACTIVITY (Corporate author)

United Aircraft Research Laboratories
East Hartford, Connecticut 06108

2a. REPORT SECURITY CLASSIFICATION

Unclassified

2b. GROUP

3. REPORT TITLE

"E-Beam HCl Laser"

4. DESCRIPTIVE NOTES (Type of report and inclusive dates)

Final Technical Report

5. AUTHOR(S) (First name, middle initial, last name)

John A. Shirley, R. J. Hall, and B. R. Bronfin

6. REPORT DATE

August 30, 1974

7a. TOTAL NO. OF PAGES

52

7b. NO. OF REFS

30

8a. CONTRACT OR GRANT NO.

N00014-72-C-0450

b. PROJECT NO.

c.

d.

9a. ORIGINATOR'S REPORT NUMBER(S)

N911340-13

9b. OTHER REPORT NO(S) (Any other numbers that may be assigned this report)

10. DISTRIBUTION STATEMENT

Distribution of this document is unlimited

DISTRIBUTION STATEMENT A
Approved for public release;
Distribution Unlimited

11. SUPPLEMENTARY NOTES

ARPA Order #1807

12. SPONSORING MILITARY ACTIVITY

Office of Naval Research
Department of the Navy
Arlington, Virgina 22217

13. ABSTRACT

The feasibility of producing stimulated emission in the 3 to 5 micron wavelength band by direct electron impact excitation of hydrogen chloride vibrational levels is being investigated theoretically and experimentally. Theoretical analysis predicts an optical gain coefficient in excess of $0.4\%cm^{-1}$. The importance of high electron density and low initial gas temperature is predicted. The results of electric discharge/laser experiments are described. Experiments have been conducted in 5% HCl/95% Argon mixtures at p=10 Torr in the e-beam sustained discharge at electron number densities up to $1.6x10^{12}cm^{-3}$. These conditions were insufficient to demonstrate stimulated emission.

DD FORM 1 NOV 65 1473 (PAGE 1)

S/N 0102-014-6600

I

Security Classification

14 KEY WORDS	LINK A		LINK B		LINK C	
	ROLE	WT	ROLE	WT	ROLE	WT
Diatomic Electric Discharge Laser						
E-Beam Excited Laser						
Hydrogen Chloride Laser						
Laser Kinetic Analysis						

II

United Aircraft Research Laboratories

UNITED AIRCRAFT CORPORATION

EAST HARTFORD, CONNECTICUT 06108

Report N911340-13

August 1974

E-BEAM HCl LASER

Final Technical Report

Sponsored by
Advanced Research Projects Agency
ARPA Order No. 1807

Monitored by
Office of Naval Research
Department of the Navy
Arlington, Virginia 22217

Contractor: United Aircraft Research Laboratories, East Hartford, Connecticut 06108
Program Code No.:
Effective Date of Contract: May 24, 1972
Contract Expiration Date: June 30, 1974
Amount of Contract: $366,022, including fee
Principal Investigator: Barry R. Bronfin (203) 565-5136

III

APPROVED BY W. G. Burwell

N911340-13

E-Beam HCl Laser

Final Report

Contract No. N00014-72-C-0450

Table of Contents

N911340-13

E-BEAM HCl LASER

I. SUMMARY

Of the infrared transmission windows existing in the sea-level atmosphere, which are of interest for Navy and DoD applications, only the 3.5 - 4.0 μ band lacks a corresponding efficient electric-discharge laser source. The research program described herein relates results of an ONR/ARPA sponsored experimental and analytical investigation of a low-pressure gaseous hydrogen chloride (HCl) medium excited by an electron-beam controlled, pulsed electric discharge to develop multiline laser emission on low-lying vibration-rotation transitions in HCl within the desired wavelength band. Consideration of reported electron swarm experiments in HCl, as well as unpublished results of low energy electron impact data, indicate that electron pumping of this molecule can be very effective at judiciously chosen discharge conditions.

The potential performance of the electrically pulsed HCl laser has been predicted theoretically. The temporal behavior of the HCl discharge medium has been analyzed from the solution of time-dependent vibrational rate equations characterizing a 0.1 - 1.0 eV plasma. Provision is made in this analysis for inelastic electron impact excitation, vibration-to-vibration and vibration-to-translation energy transfer, spontaneous and stimulated emission and electron dissociative attachment.

These calculations indicate that this system should be characterized by optical gains in excess of 0.4% cm^{-1} on the $v=5 \rightarrow 4$ bands of HCl. Efficient laser action, however is predicted to occur only when the electron number density is considerably in excess of $10^{12} cm^{-3}$, and only if the initial gas temperature is at least as low as 200°K. The theoretical analysis indicates that neither dissociative attachment nor the fast vibrational relaxation of HCl should prevent lasing from occurring.

Pulsed electric discharge laser tests have been performed using a UARL 5 cm^2 electron gun to ionize a high aspect ratio discharge in a longitudinal configuration. Neither stimulated emission nor spontaneous emission has been observed from HCl vibrational transitions in the 5% HCl/95% Argon mixture discharges at 10-15 Torr pressure and room temperature. Electron number densities in the plasma $\leq 1.6 \times 10^{12} cm^{-3}$ have been deduced from a consideration of the calculated electron drift velocity in the HCl/Ar mixture and the measured sustainer current. The reduced electric field applied was between 3×10^{-17} and 3×10^{-16} V-cm^2. Experimental conditions were insufficient to sustain population inversions large enough to exceed laser cavity threshold conditions. The electron densities sustained were limited by severe electron beam losses occurring at the foil/gas interface in these experiments. Methods of limiting the effects of beam scattering should prove beneficial to HCl e-beam laser technology.

II. INTRODUCTION

Since mid-April 1972 the United Aircraft Research Laboratories (UARL) have been engaged in a research program sponsored by ONR/ARPA, under Navy Contract N00014-72-C-0450 (Ref. 1) to explore the possibility of generating stimulated emission from the vibrational-rotational transitions of hydrogen chloride excited in an electron-beam controlled electric discharge.

An efficient source of coherent radiation in the 3.5 - 4.0 μ atmospheric transmission window would prove interesting for several Navy and DoD applications. Prior to the initiation of the present investigation the only sources in this wavelength region were hydrogen chloride (HCl) and deuterium fluoride (DF) chemical lasers. In addition to their often low efficiencies, the operation of chemical lasers also suffer the disadvantages of requiring the operator to deal with the storage, disposal and resupply of highly toxic and extremely reactive fuels. The fully developed HCl or DF electrically-pumped laser could be envisioned to operate free of any chemical reaction in a closed cycle, thereby obviating disposal and resupply problems.

Theoretical studies (Ref 1) conducted before the Contract award had indicated the possibility of laser action in hydrogen chloride pumped by electron impact; however, these calculations also indicated that careful control of experimental parameters would be necessary for a successful demonstration. For these reasons, a combined theoretical and experimental investigation of HCl excited by a pulsed discharge, sustained by a pulsed electron beam, was proposed and was pursued in the subject research program. Subsequent investigations (Ref. 2 and 3) have indicated the likelihood of strong vibrational excitation by electron impact in HCl. Results obtained at other laboratories (Ref. 4 and 5) have shown vibrational excitation and development of stimulated emission from the analogous hydrogen halides: HF and DF. These results have been summarized in Ref. 2.

The theoretical model descriptive of the HCl electric-discharge laser medium and results derived therefrom are presented in Section III. The experimental apparatus and the results of experiments conducted are discussed in Section IV. Finally conclusions are drawn in Section V.

III. THEORETICAL INVESTIGATIONS

The aim of our theoretical investigations has been to determine (1) whether the HCl vibrational degree of freedom can be excited efficiently in an electron-beam sustained electric discharge, and (2) whether anharmonic pumping due to HCl VV exchange can offset parasitic VT decay to yield measurable laser gain and power. Our approach has been to solve the time-dependent kinetic master equations governing the rates of change of HCl vibrational state densities under the influence of the following processes (1) pumping due to electron impact (2) single-quantum VV exchange (3) single quantum VT relaxation and (4) single-quantum stimulated emission. The ranges of experimental parameters considered in our computer simulations were those determined by the constraints of the existing experimental apparatus.

Electron-Molecule Excitation Rates

Analytical prediction of electrically-excited HCl laser performance requires a reasonable estimate of the cross sections for vibrational excitation of HCl via electron impact. Therefore, considerable analytical effort has been devoted to the theoretical interpretation of the experimental transport data appearing in the literature descriptive of electron-HCl collisional interactions (Ref. 6). These analyses were conducted to reveal as much as possible regarding the electron-HCl vibrational excitation process. The cross-sections inferred from these analyses were subsequently corroborated by the results of electron transmission experiments conducted by Professor G. Schulz's laboratory at Yale University (Ref. 3). The transport data analysis and the transmission experiments both indicate a peak value of about $1.5 \times 10^{-15} cm^2$ for the cross section for excitation of the first HCl vibrational state.

The early electron-HCl transport data of Bailey and Duncanson (Ref. 7) indicate unusually large electron energy losses in HCl for characteristic electron energy values below 1.0 eV. Reasonable estimates of the electron drift velocity v_d and characteristic electron energy ϵ_K can be deduced from this data as a function of the Townsend parameter. Using these data in conjunction with other techniques (Ref. 8), the Frost and Phelps technique (Ref. 9) for the analysis of transport coefficients was used to determine a self-consistent set of electron-HCl cross sections.

Analysis of the Bailey and Duncanson transport data requires numerical solution of the electron Boltzmann equation using a complete trial set of HCl cross sections. The computed electron energy distribution function is then used to calculate the electron drift velocity and characteristic energy which are compared with experimental data. Adjustments are made to the initial cross section set in a trial and error fashion until the calculated and experimental transport data are in reasonable agreement (Fig. 1). This technique has lead to the self-consistent set of electron-HCl cross-sections shown in Fig. 2. As indicated, the cross-section for excitation of the first vibrational level reaches a value in excess of $1.5 \times 10^{-15} cm^2$ slightly above threshold. Also shown in Figure 2 are the various contributions to the momentum transfer cross section, Q_m, the cross section for HCl dissociative attachment, and an effective electronic cross section which is most likely related to the direct dissociation process.

COMPUTED e-HCl TRANSPORT COEFFICIENTS

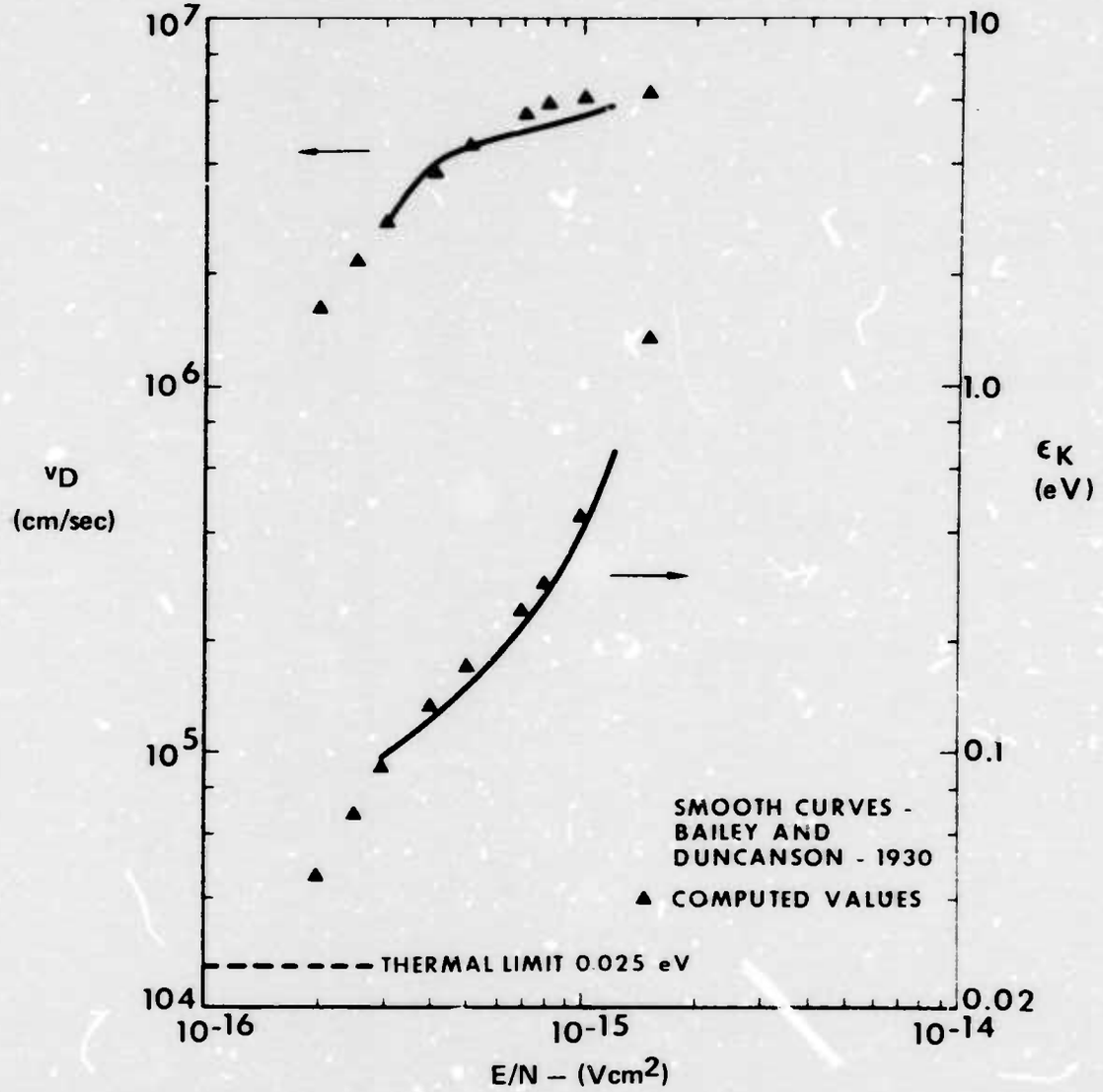

United Aircraft Research Laboratories

N911340–13

FIG. 1

FIG. 2

PRELIMINARY HCl CROSS SECTIONS

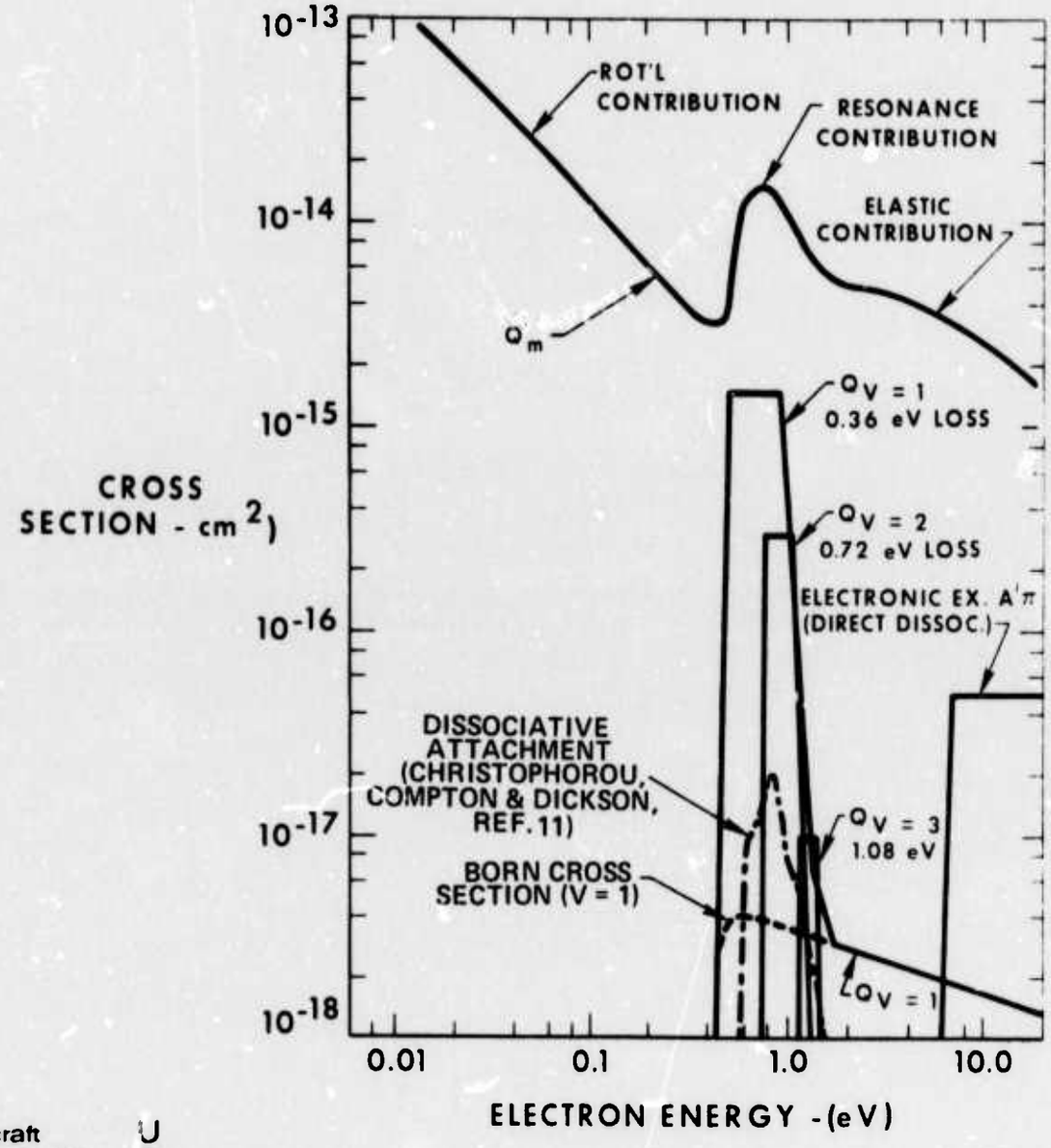

United Aircraft Research Laboratories

The set of cross-sections presented in Fig. 2 can be used in conjunction with the calculated electron distribution function to determine the fractional power transfer to the various energy loss channels. Figure 3 presents the results of such a calculation as a function of E/N for a 1:9 HCl:He mixture. The fractional power transfer curves for HCl:Ar mixtures are quite similar. Vibrational excitation of HCl is predicted to be quite efficient for $0.15 < \epsilon_K < 0.75$ eV.

Integration of the distribution function and loss process cross sections results in the rate coefficients for these processes (Fig. 4). As can be seen, the rate coefficient for dissociative attachment is predicted to be more than two orders of magnitude smaller than that for excitation of the first vibrational level, which has a relatively constant value of about $10^{-8} cm^{-3}$/particle/sec.

A series of electron transmission experiments are underway within Professor George Schulz's laboratory at Yale University (Refs. 3 and 10). These experiments have included an investigation of HCl in which the presence of a series of large resonances at low electron energies ($\epsilon_K < 5$ eV) has been detected. Ziesel and Schulz (Ref. 3) have been able to deduce cross-sections for excitation of HCl(v=1) and HCl(v=2) normalized to the absolute cross section for dissociative attachment. Using the dissociative attachment cross-section reported by Christophorou et al. (Ref. 11), they calculate that the peak of the HCl(v=1) cross-section is about 1.5×10^{-15} cm^2, in excellent agreement with the value inferred by the UARL analysis of the Bailey and Duncanson transport data. Because the later analysis also used the Christophorou cross section, the results of Yale experiments and the UARL calculations are consistent. Because the magnitude of the vibrational excitation cross section cannot be accounted for by direct excitation processes, the Yale group assumes that excitation proceeds by a resonant process involving $HCl^-(^2\Sigma^+)$.

Discharge Model

The state of the plasma is assumed to be specified by the initial values of electron number density, Townsend parameter, and neutral composition. Changes in the electron distribution function resulting from electron encounters with vibrationally-excited HCl are assumed to be small. This assumption is thought to be valid since the electron "temperature" typically is much greater than a vibrational "temperature" characteristic of the lower, more populous HCl states. Further, the fraction of HCl dissociated during the electron pulse is small as will be shown. The electron pulse is treated mathematically as square

$$n_e = n_e \quad 0 \le t \le \tau,$$

$$= 0 \qquad t > \tau$$

An attachment-dominated plasma is assumed, so that n_e is not affected by changes in total gas density due to heating. The heavy-particle translational/rotational temperature rise is calculated from the simple relation

$$\frac{dT}{dt} = \frac{Q}{\rho C_p}$$

FIG. 3

FRACTIONAL POWER TRANSFER IN HCl–He MIXTURE

HCl:He = 1:9

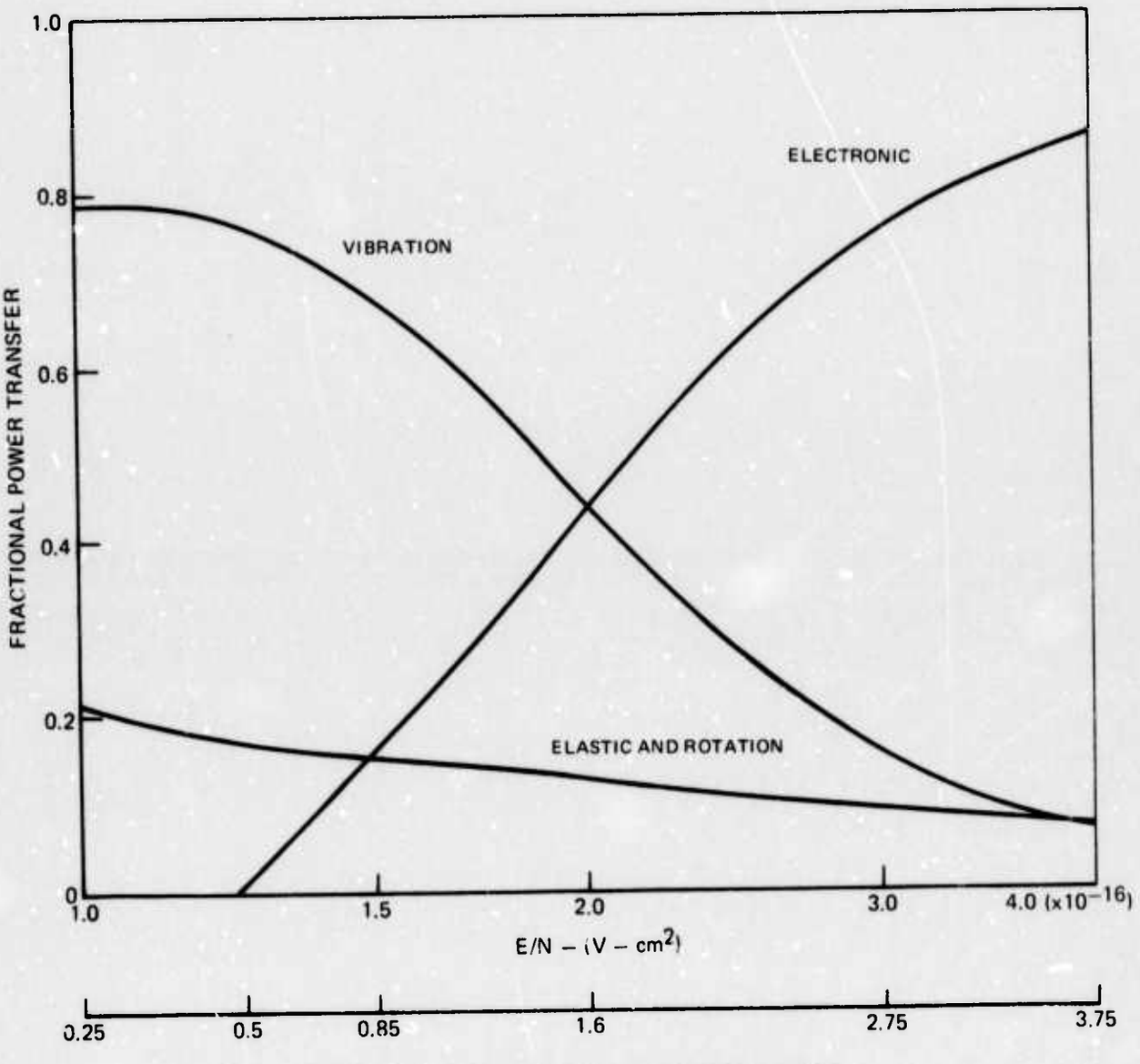

N07-1-1

FIG. 4

CALCULATED ELECTRON–MOLECULE RATE COEFFICIENTS

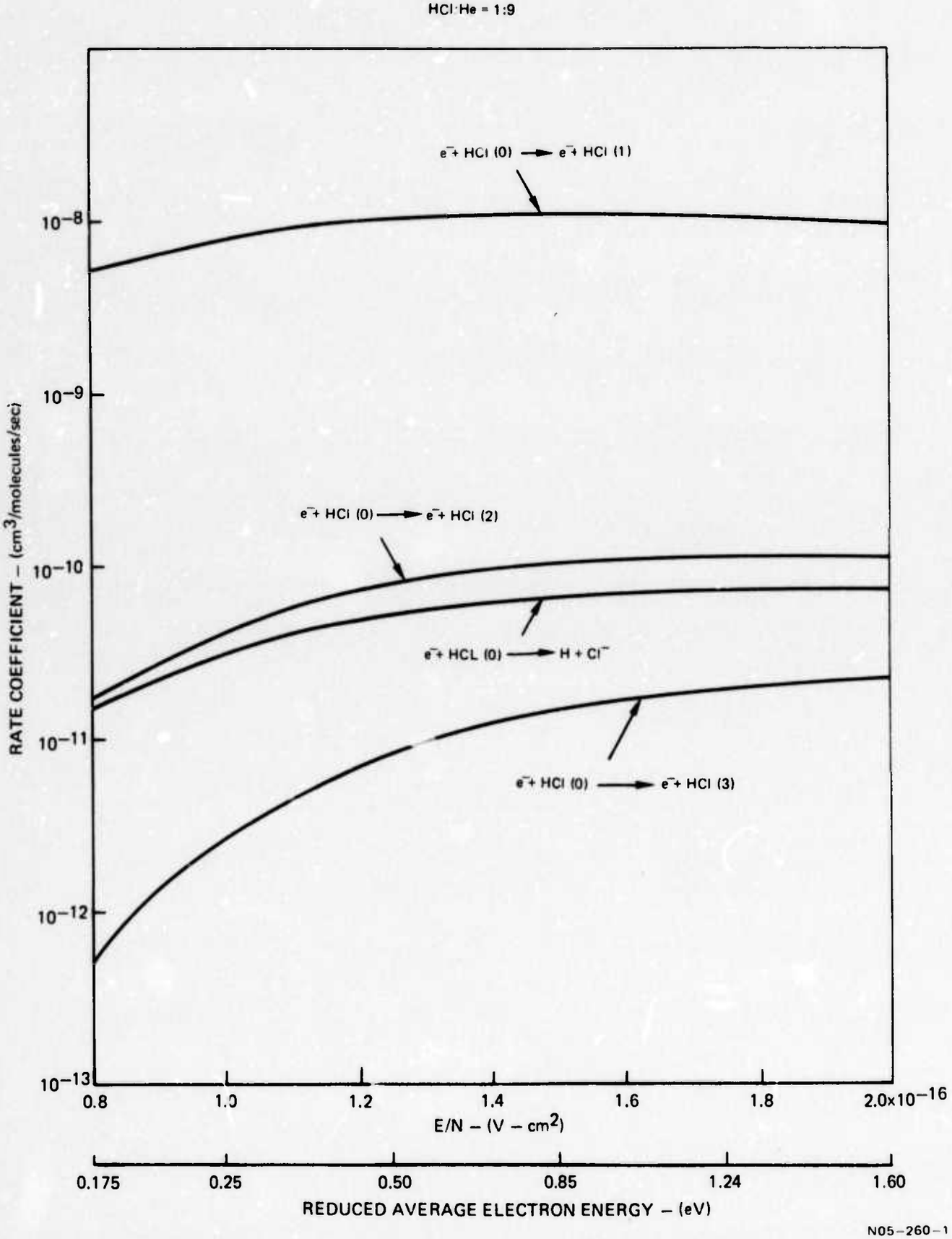

where Q represents the volume rate of translational/rotational heating due to elastic-rotation electron energy loss, vibrational relaxation (primarily VT) and stimulated emission (P-branch emission results in a rotational energy increase); C_p is the effective heat capacity per unit mass

$$C_p = \frac{\gamma}{\gamma-1}\frac{R}{\tilde{M}}$$

where γ is the frozen ratio of specfic heats of the gas, R is the universal gas constant, and $\tilde{M}$ the average molecular weight; and ρ is the mass density of the gas.

Becasue H and Cl atoms are efficient deactivators of HCl(v) (Refs. 12 and 13), and because the peak in the dissociative attachment cross section occurs at an electron energy near that for HCl vibrational excitation, estimation of the atom concentrations constitutes an important part of the analysis. The master equations include terms representing chemical changes due to the processes

Dissociative attachment: $e^- + HCl(v) \xrightarrow{K_1} H + Cl^-$ (1)

Reverse pumping reaction: $H + HCl(v) \xrightarrow{K_2} H_2 + Cl$ (2)

The process

$$Cl + HCl(v) \rightarrow H + Cl_2$$

is substantially endothermic for $v \leq 6$; because only a small fraction of HCl molecules reside in quantum states beyond v=6, the time scale for this reaction will be longer than those for (1) and (2).

The rate coefficients for (1) and (2) are assumed to be independent of quantum number. For process (1) it is unclear how to model the effect of target HCl vibration; for process (2), the experimental results of Ref. 12 indicate that HCl vibrational excitation has no effect on reaction rate constant. Therefore (Ref. 12),

$$K_2(v) = 4.2\times10^{-11}\exp\left(\frac{-3500}{RT}\right) \quad v=0,\ 1,\ 2\ \ldots$$

HCl-HCl VV Rates

The rate coefficient for the process

$$HCl(2) + HCl(0) \overset{P^{0,1}_{2,1}}{\rightarrow} 2\ HCl(1)$$

has been measured by several investigators (Refs. 15 and 16). The average of the room temperature values reported is about $2.75 \times 10^{-12} cm^3$/molecule/sec. Further, it has been established that the rate coefficient varies as $T^{-\frac{1}{2}}$ for the temperature range of interest (Ref. 14). Accordingly, the scaling of these rates employs a simple function whose form is suggested by the Sharma theory (Refs. 17 and 18).

$$\frac{P^{s,s+1}_{r,r-1}}{P^{0,1}_{1,0}} = \frac{r(s+1)(1-\epsilon)^2}{(1-r\epsilon)[1-(s+1)\epsilon]} \exp\left(\frac{\Delta E^{s,s+1}_{r,r-1}}{2kT}\right) \exp\left[-\left(\frac{\Delta E^{s,s+1}_{r,r-1}}{\delta}\right)^2\right]$$

where

$$P^{0,1}_{1,0} = \frac{C}{\sqrt{T}}$$

ϵ is the molecular anharmonicity, and C is a numerical constant and ΔE is the overall energy defect of the reaction. The unknown parameter δ governs the effect of reaction non-resonance on reaction rate. It would be used to fit the theoretical expression to experimental data for

$$HCl(v) + HCl(0) \rightarrow HCl(v-1) + HCl(1) \qquad v > 2$$

However, only limited and approximate data exist for these processes (Ref. 19), so δ must be estimated. A value of 10^{-13} ergs gives rise to the VV rate matrix shown in Figure (5). For $\delta = 10^{-13}$ we have the physically resonable relationship

$$\frac{P^{0,1}_{r,r-1}}{P^{0,1}_{r-1,r-2}} \approx \frac{1}{2} \text{ at } T = 300^\circ K$$

VT Rates

Of the chemical species likely to be present in the HCl discharge, only H, Cl (Cl^-), and HCl itself will make an appreciable contribution to HCl VT relaxation. The time constant for the relaxation of HCl(v=1) by HCl has an inverse temperature dependence below 300°K with values of about 1.6 μsec atm at 300°K and .25 μsec atm at 150°K (Refs. 20 and 21). For H-atom relaxation of HCl(1) a time constant value at room temperature of about 6×10^{-9} sec-atm can be inferred from the work of Ref. 12. For Cl atom deactivation, there is a large disparity between the two reported rates Ref. 13 and 22. The faster rate, 4×10^{-9} sec-atm, is judged to be the more accurate. Because the investigators (Ref. 22) now believe that this rate is about a factor of two too fast, a value of 8×10^{-9} sec-atm has been used. The time constants for VT deactivation by both H and Cl are assumed to be temperature independent in the range $150 < T < 300^\circ K$. Cl^- is assumed to be as efficient a VT deactivator as Cl. The scaling of VT rate constants with quantum number is essentially harmonic:

FIG. 5

HCl–HCl VV AND VT RATE MODELS

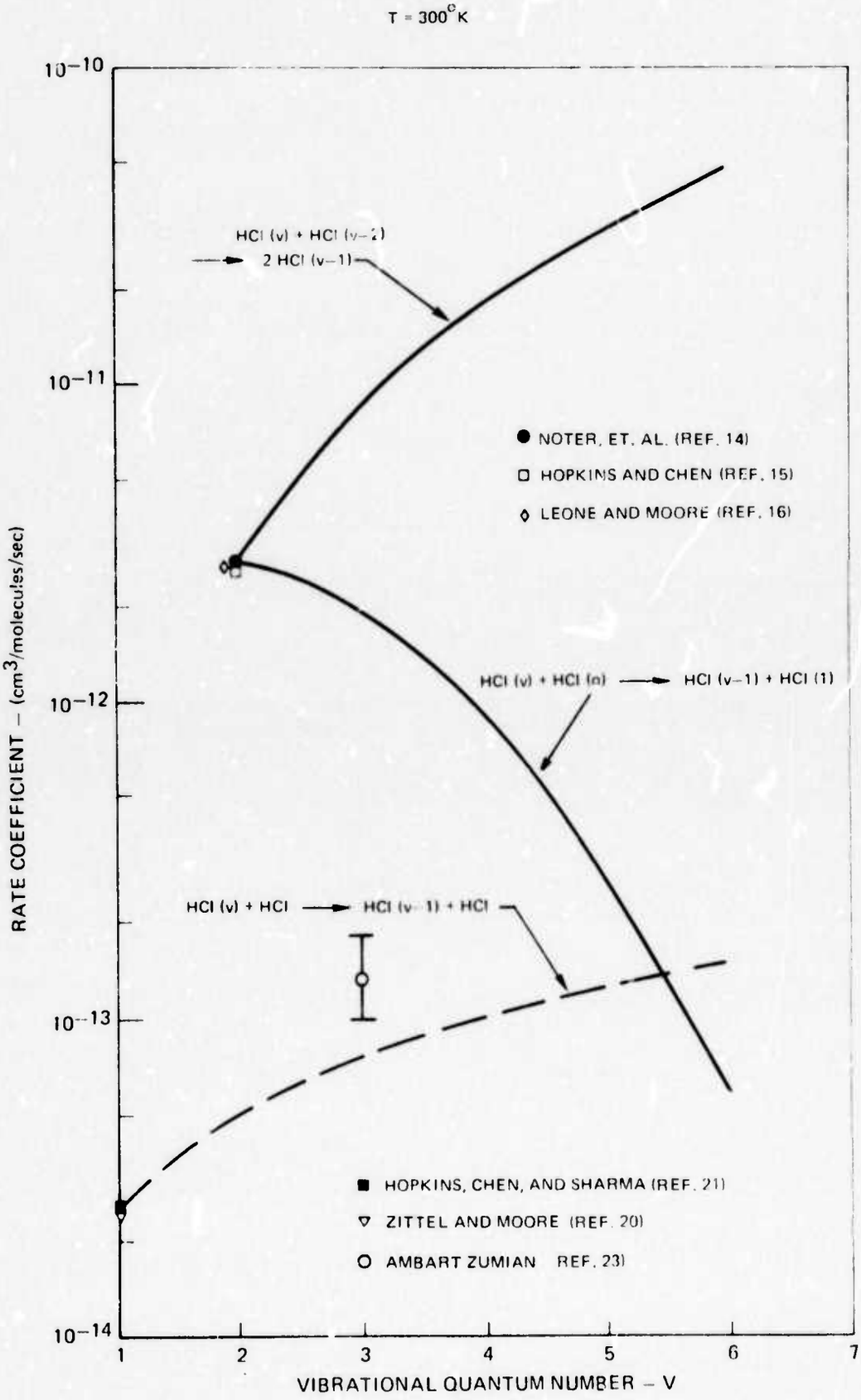

N06-109-1

$$\frac{Q_{r,r-1}}{Q_{1,0}} = \frac{r(1-\epsilon)}{(1-r\epsilon)}$$

where $Q_{r,r-1}$ governs the rate for

$$HCl(r) + M \rightarrow HCl(r-1) + M$$

Calculational Procedure

The kinetic rate equations for the chemical compositions, vibrational populations, and bulk gas properties (T,N, . . .) form a coupled equation set which can be expressed in the following form

$$\frac{dy_r}{dt} = F_r\,(y_s)$$

where y_r is the unknown vector. The finite-difference approximation used to solve this equation is:

$$y_r^{(j+1)} = y_r^{(j)} + \Delta t F_r(\bar{y}_s)$$

where

$$\bar{y}_s = \tfrac{1}{2}\left(y_s^{(j+1)} + y_s^{(j)}\right)$$

$$\Delta t = t^{(j+1)} - t^{(j)}$$

and the superscript denotes the integration step number. This implicit equation is solved by an iterative procedure. The local step size is determined from the relation.

$$\Delta t = K\max\left[\frac{y_r^{(j)}}{F_r(y_s^{(j)})}\right]$$

where K is a constant that is $\approx 10^{-2}$.

Stimulated Emission

In the computer code, lasing is assumed to initiate when the peak P-branch gain on a particular vibrational transition reaches the cavity threshold value

$$g_{osc} = -\frac{1}{2L}\ln(R_1R_2)$$

where L is the length of active medium between the mirrors, and the R's is the reflectivity of mirror i. The local optical power density on this transition is

$$g_{osc} \, I^{v,J_{max}}_{v-1,J_{max+1}}$$

where $I^{v,J_{max}}_{v-1,J_{max+1}}$ is the total optical flux on the transition determined from the constraint that

$$g(v,J_{max} \rightarrow v-1,J_{max+1}) = g_{osc}$$

Rotational equilibrium is assumed in the laser cavity, even though the lines will be primarily Doppler-broadened for our experimental conditions.

Calculated Results

Computed small-signal gain profiles for a representative set of experimental conditions are presented in Fig. 6. The gas is assumed to have been chilled to 200°K. Positive gain lifetimes of several hundred microseconds are predicted, with the (4-3), (5-4), and (6-5) transitions having a maximum gain of approximately 0.5%/cm. The gain rise time for these lines is about 100 μsec. The predicted gain on the low-lying transitions (3-2 and below) is quite small.

As seen in Fig. 7, the calculated mole fractions of H and Cl atoms will be about 10^{-3} that of HCl for a typical set of conditions. Taking into account the relative magnitudes of the time constants for VT relaxation (see discussion of VT rates) it can be concluded that the rate of HCl VT deactivation by atomic species will not exceed the rate of self-relaxation.

The extreme sensitivity of small-signal gain to electron number density is shown in Fig. 8. At 200°K, an electron number density of $10^{12}cm^{-3}$ produces gains slightly in excess of 0.001 cm^{-1}. An electrical power per unit volume a factor of two higher leads to calculated gains near .01 cm^{-1}. At 300°K, on the other hand, an electron number density of $3x10^{12}$ is needed to produce gains in excess of 0.001 cm^{-1} (Fig. 9). A value of $1.5x10^{12}cm^{-3}$ results in a gain that does not exceed typical threshold gains. The strong sensitivity of gain to translational temperature is primarily due to enhancement of anharmonic pumping as the gas is cooled. It appears that the peak gain is approximately proportional to the initial partical pressure of HCl for a fixed electron density (Fig. 10). The gain lifetime is inversely proportional to the initial HCl partial pressure.

Further increases in gain can be achieved by initital temperature reduction to 150°K (Fig. 11). Even though the rate constant for HCl self-relaxation is increasing rapidly as the temperature is reduced in this regime, stronger anharmonic pumping, reduced gain line widths, and a more favorable rotational distribution lead to markedly increased gains relative to 200°K.

The variation of gain with pulse width and HCl mole fraction is presented in Figs. 12 and 13. These results are consistent with the following relation-

FIG. 6

CALCULATED GAIN COEFFICIENTS IN PULSED HCl ELECTRIC DISCHARGE LASER

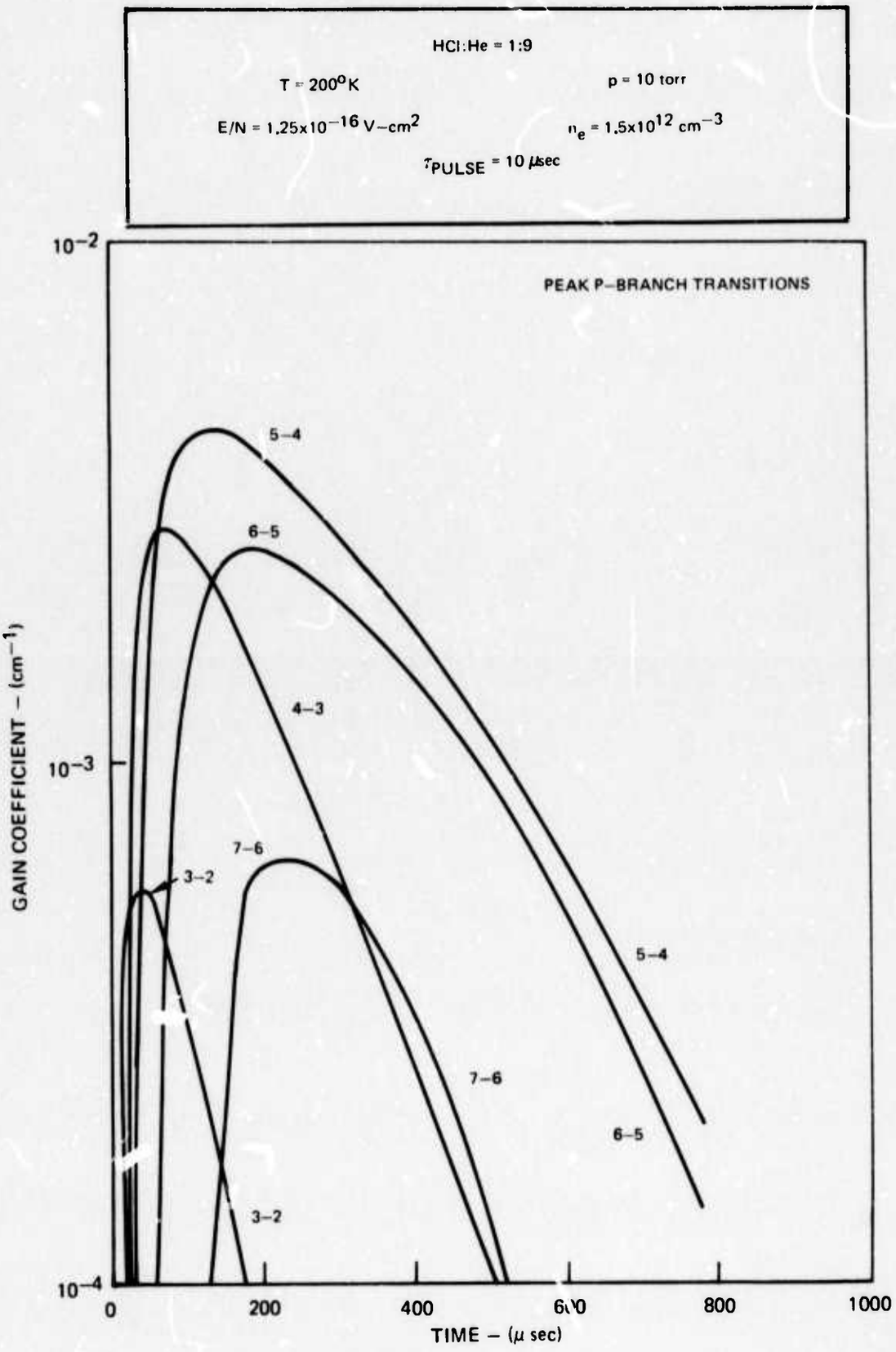

N06–71–6

FIG. 7

CALCULATED SPECIES PROFILES IN HCl EDL

HCl: He = 1:9

p = 10 torr T = 200°K

E/N = 1.25×10^{-16} V – cm^2 $n_e = 2 \times 10^{12}$ cm^{-3}

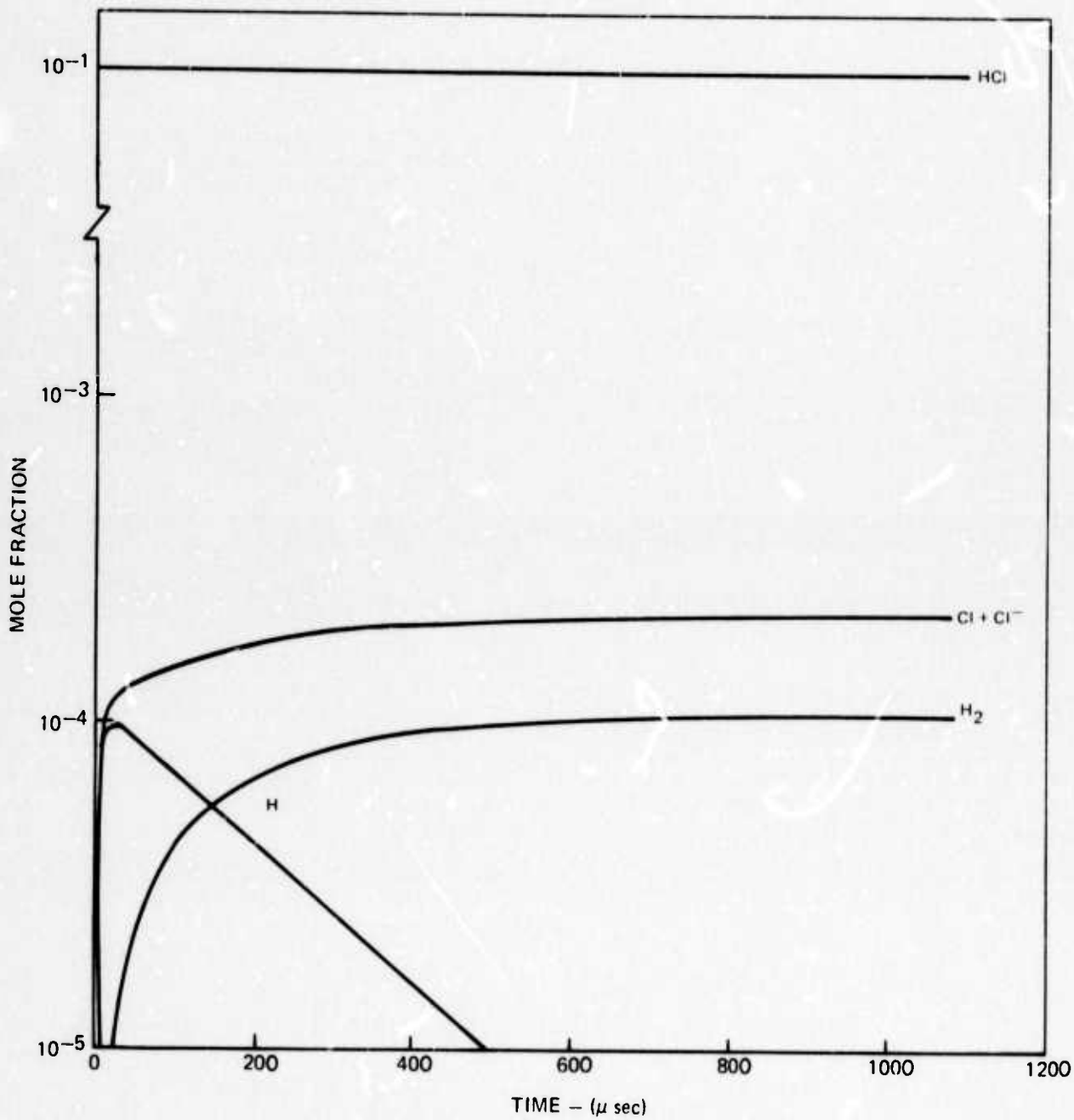

N05–260–2

FIG. 8

VARIATION OF CALCULATED HCl (5→4) GAIN COEFFICIENT WITH ELECTRON NUMBER DENSITY

HCl:He = 1:9

p = 10 torr

T = 200°K

E/N = 1.25×10^{-16} V–cm^2

τ_{PULSE} = 10 μsec

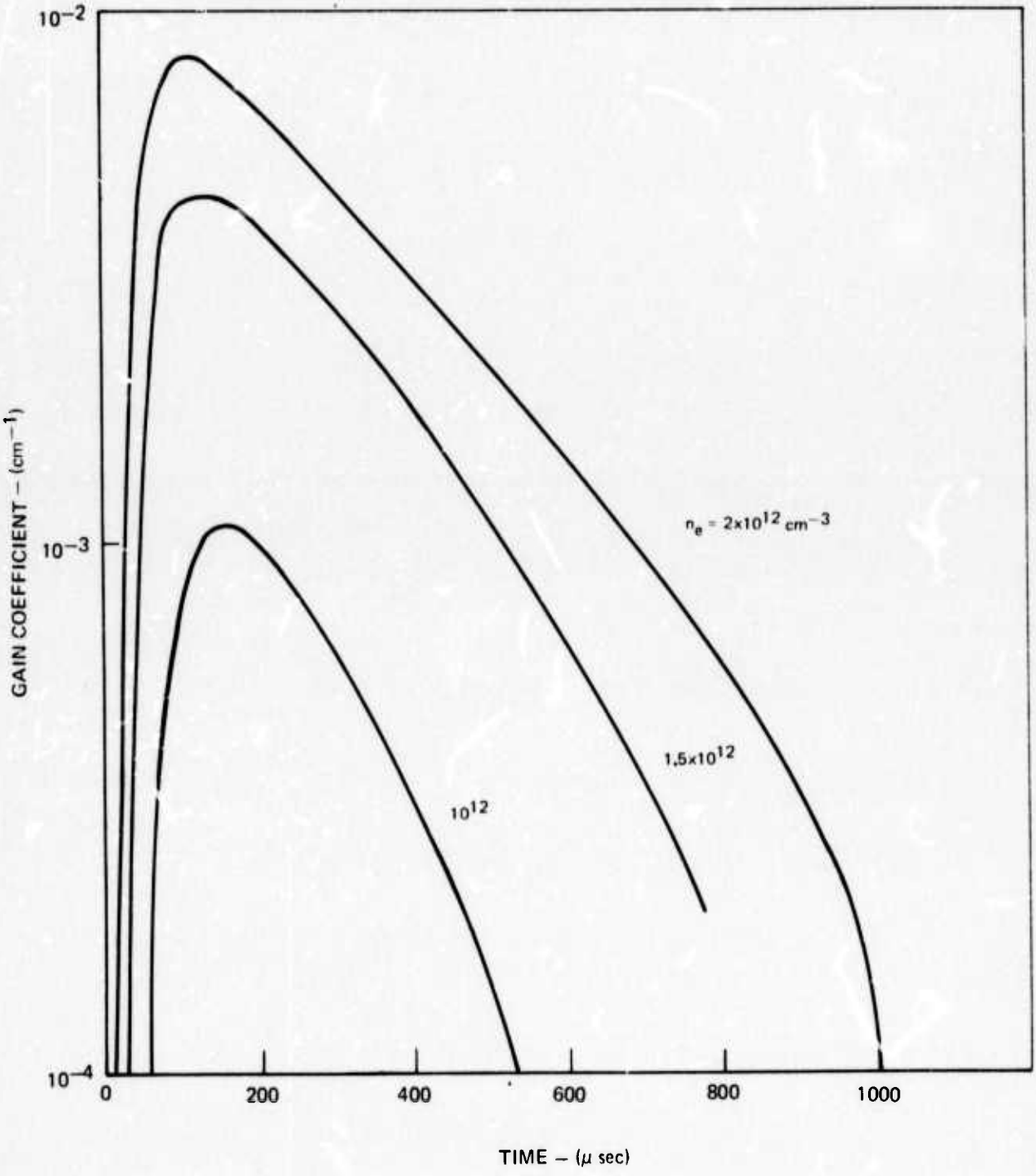

N06-71-3

N911340–13

CALCULATED VARIATION OF HCl (6–5) GAIN COEFFICIENT WITH ELECTRON NUMBER DENSITY

FIG. 9

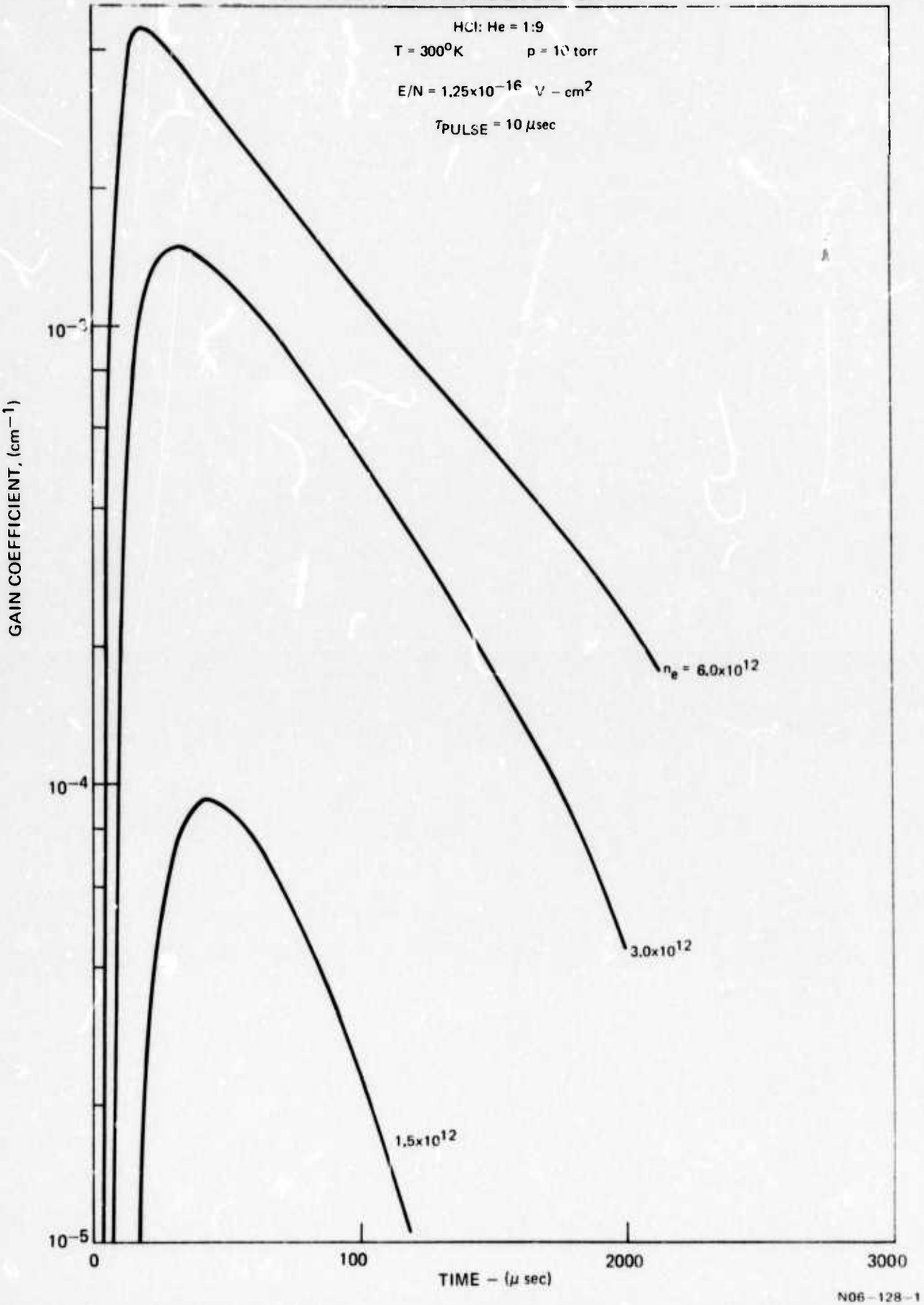

FIG. 10

VARIATION OF CALCULATED HCl (5–4) GAIN COEFFICIENT WITH GAS PRESSURE

HCl:He = 1:9 $\quad T = 200^{o}K$

$E/N = 1.25 \times 10^{-16}$ V–cm^2 $\quad n_e = 1.5 \times 10^{12}$ cm^{-3}

$\tau_{PULSE} = 10\ \mu$sec

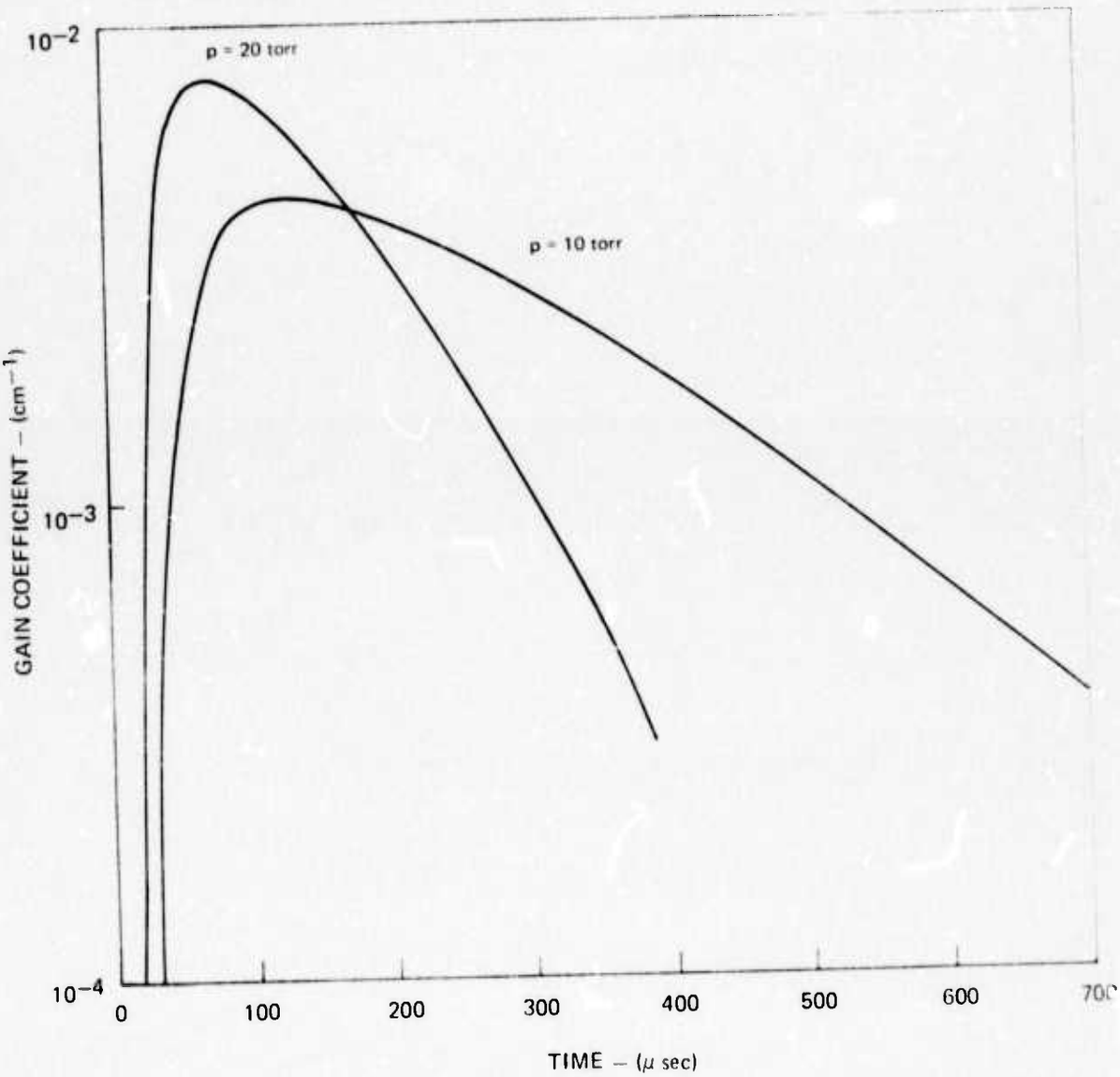

N06-71-4

FIG. 11

CALCULATED VARIATION OF HCl (5–4) GAIN COEFFICIENT WITH INITIAL TRANSLATIONAL – ROTATIONAL TEMPERATURE

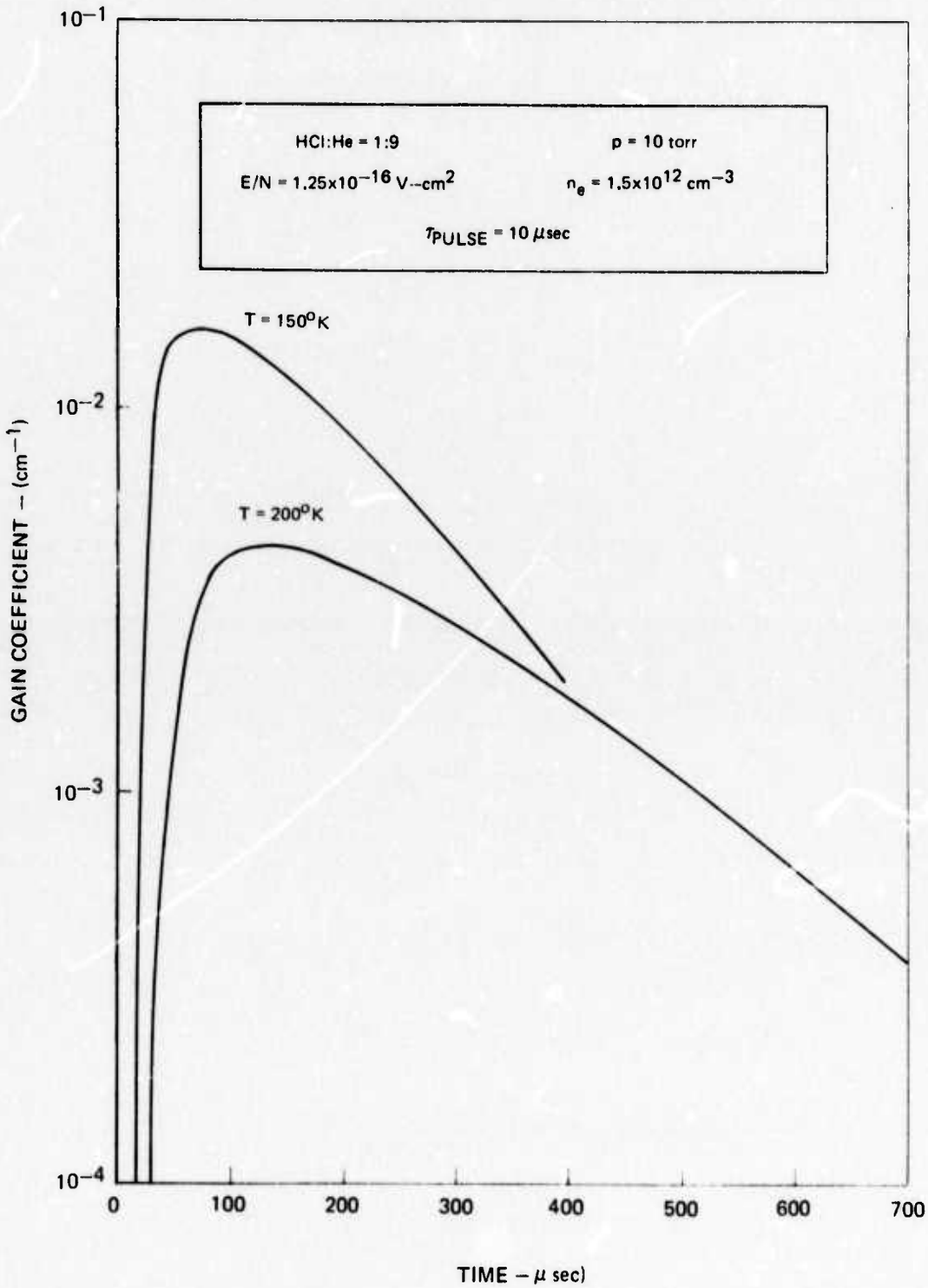

N06–71–1

FIG. 12

CALCULATED VARIATION OF HCl (5 – 4) GAIN COEFFICIENT WITH PULSE WIDTH

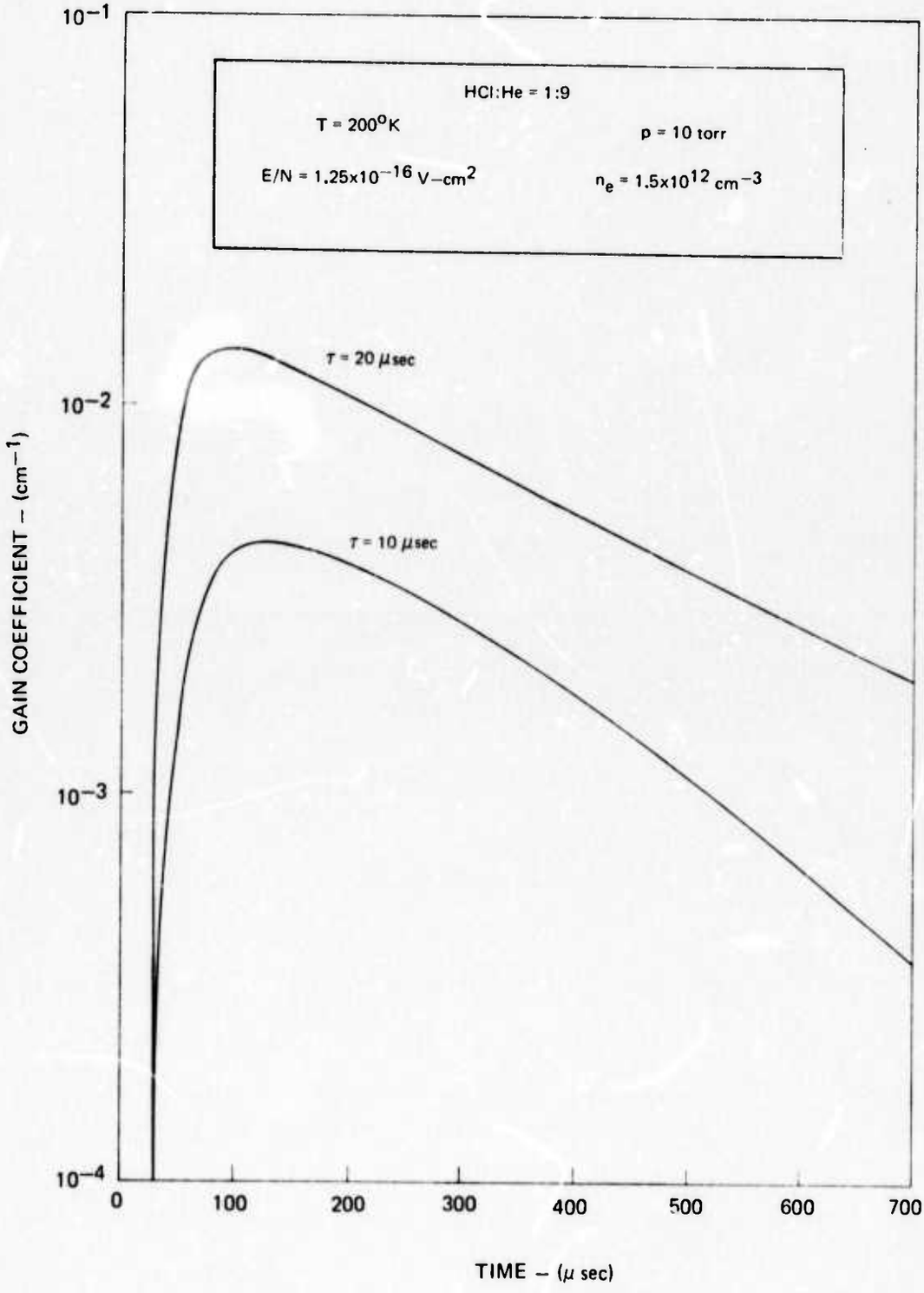

N06–71–2

FIG. 13

VARIATION OF CALCULATED HCl (5–4) GAIN COEFFICIENT WITH MOLE FRACTION OF HCl

$T = 200^{o}K$	$p = 10$ torr
$E/N = 1.25 \times 10^{-16}$ V – cm^2	$n_e = 1.5 \times 10^{12}$ cm^{-3}
$\tau_{PULSE} = 10\ \mu$ sec	

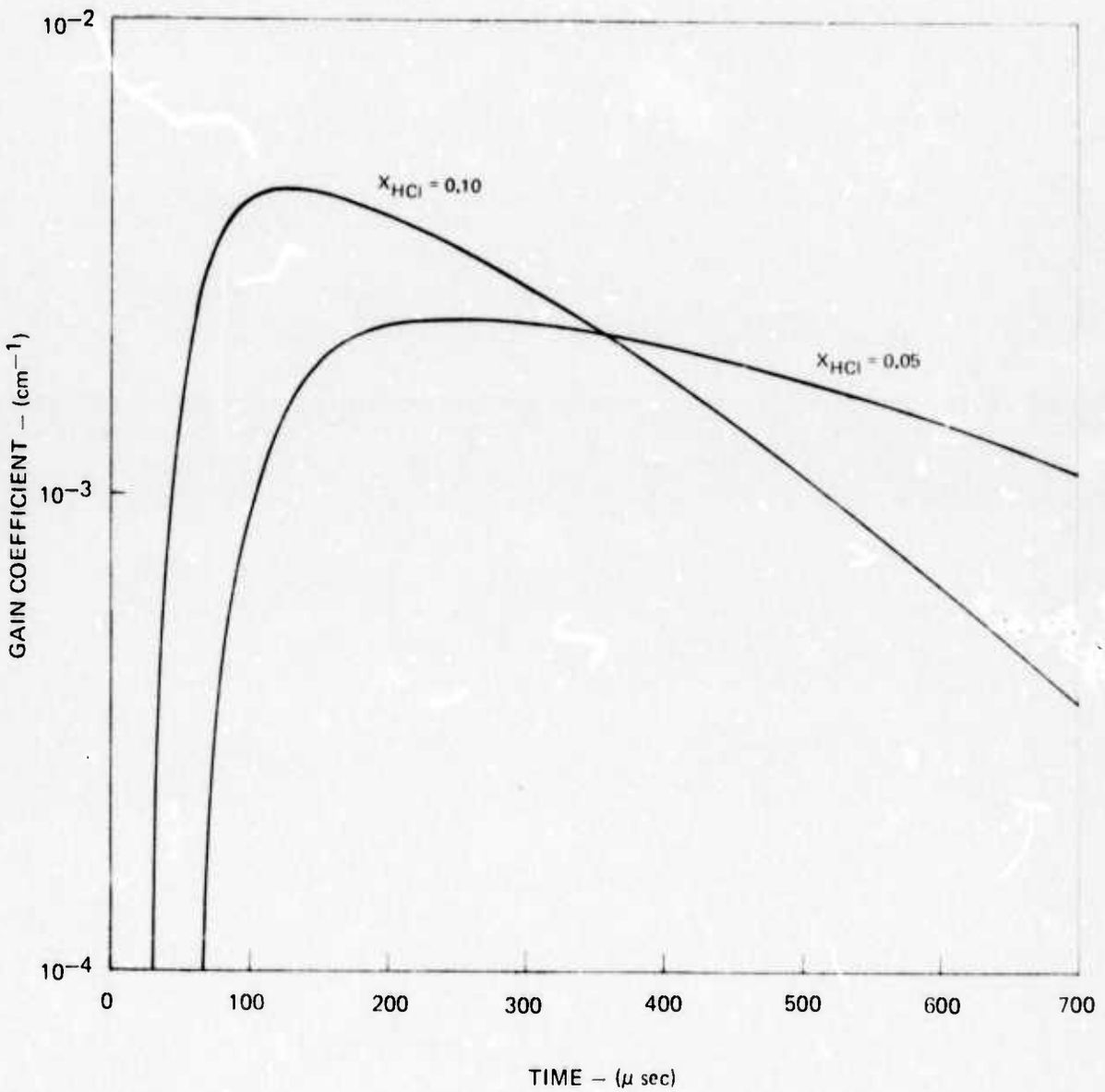

N06-71-7

ship between peak gain (g_o), electron number density (n_e), partial pressure of HCl (p_{HCl}) and pulse width (τ)

$$g_o \propto n_e p_{HCl}$$

which is indicated by the results of the computer analysis.

It is of interest to examine the cumulative energy balance in the presence of lasing (Fig. 14). For the conditions shown, about 60 kJ/lb is deposited in vibration. Spontaneous emission and VV processes remove only a small amount of vibrational energy, but the energy loss due to VT relaxation exceeds that due to lasing. The overall efficiency for this case is about 11-12%.

The calculated overall efficiency also has a strong dependence on translational temperature, as can be seen in Fig. 15. At 200°K, electron number densities near $4x10^{12}cm^{-3}$ are predicted to produce efficiencies in excess of 20% and powers in excess of 250 joules/liter/atm_{HCl}. At 300°K, on the other hand, an electron density of $2x10^{12}cm^{-3}$ is just sufficient to exceed cavity threshold; at $4x10^{12}$, an efficiency of only 5% is predicted.

The variation of spectral power output with electron density is shown in Fig. 16. With $n_e = 2x10^{12}cm^{-3}$ the dominant transition is the 3-2, followed by the 4-3 and 5-4 transitions. The power output is consequently in the wavelength range 4-4.4 microns. At $n_e = 4x10^{12}cm^{-3}$, the dominant V-V transition is still 3-2; however, substantial power is extracted from the 1-0 and 2-1 transitions. Because the emission from these lines occures during and immediately after the electron pulse, it can be concluded that direct electron pumping is the cause of the inversion of these lines.

Sensitivity of Calculations to Assumed Rates

That the calculated gain is strongly dependent on the rate coefficient for electron pumping of the HCl can be inferred from Figs. 8 and 9. The calculated results depend on the product of rate coefficient and electron number density; thus a variation in rate constant at fixed n_e is equivalent to the variation of n_e at fixed rate constant. (Figs 8 and 9).

These theoretical results are also strongly dependent on the form of the VV rate matrix. Increasing the parameter δ by a factor of 5 shifts the gain distribution toward higher quantum numbers. Decreasing δ by a factor of 5 leads to a prediction of negligible gain. The latter rate matrix is felt to be physically unrealistic, however; it is thought that the actual rate matrix is described by a value of δ in the range 1 to 5 times the nominal value.

Variations in the VT rates were not undertaken, because the HCl self-relaxation rate appears to have been measured quite accurately, and the atomic deactivation rates used approach gas kinetic values. However, if the scaling of VT rates is considerably faster than the harmonic model, or if multiple-quantum processes are important, the predictions of population inversion would be questionable.

FIG. 14

CUMULATIVE ENERGY BALANCE IN HCl EDL

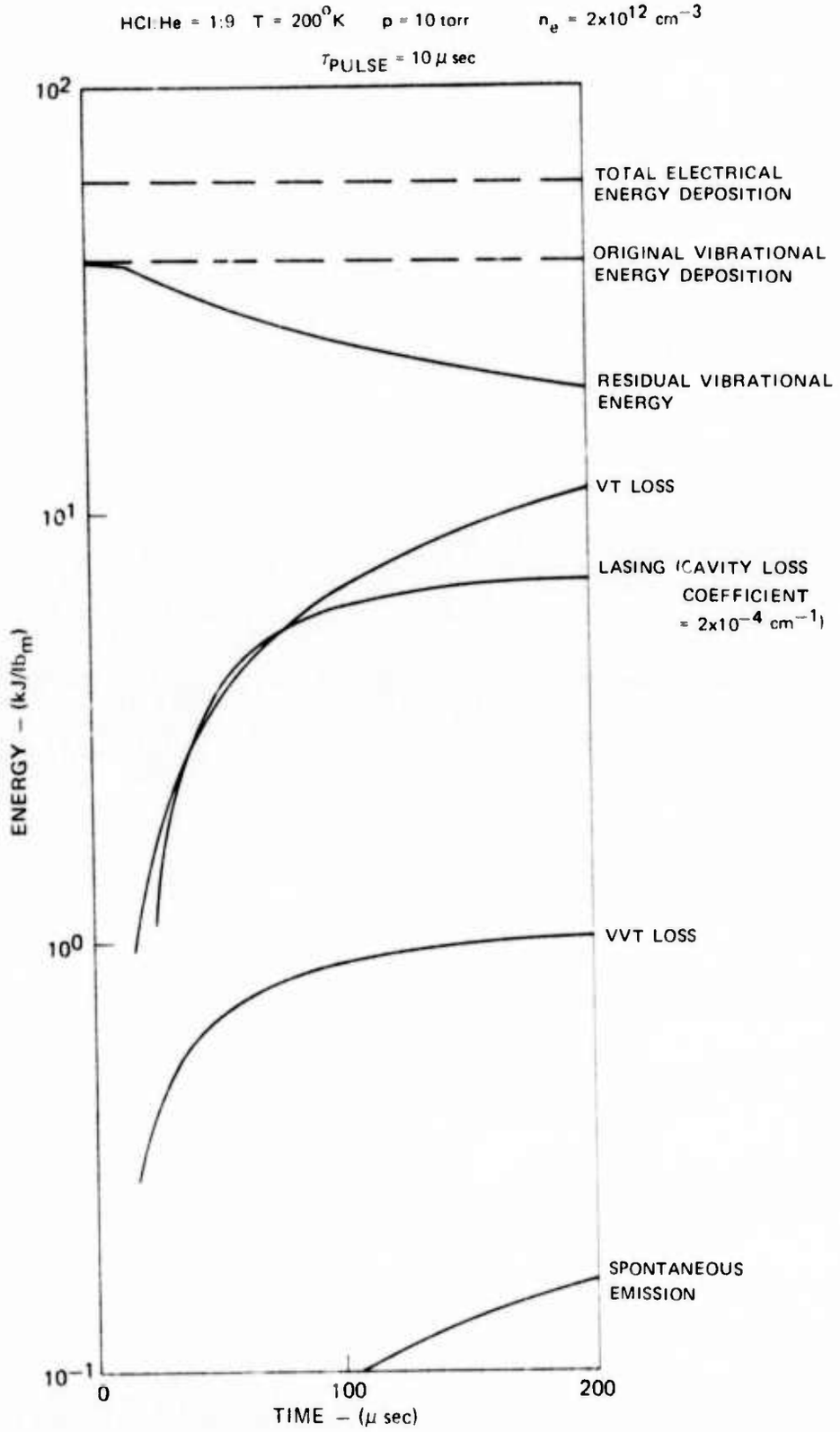

N06-200-2

CALCULATED OVERALL EFFICIENCY IN PULSED HCl EDL

HCl: He = 1:9 $\quad E/N = 1.25\times10^{-16}$ V–CM^2

p = 10 TORR $\quad \alpha_{CAV} = 2\times10^{-4}$ CM^{-1}

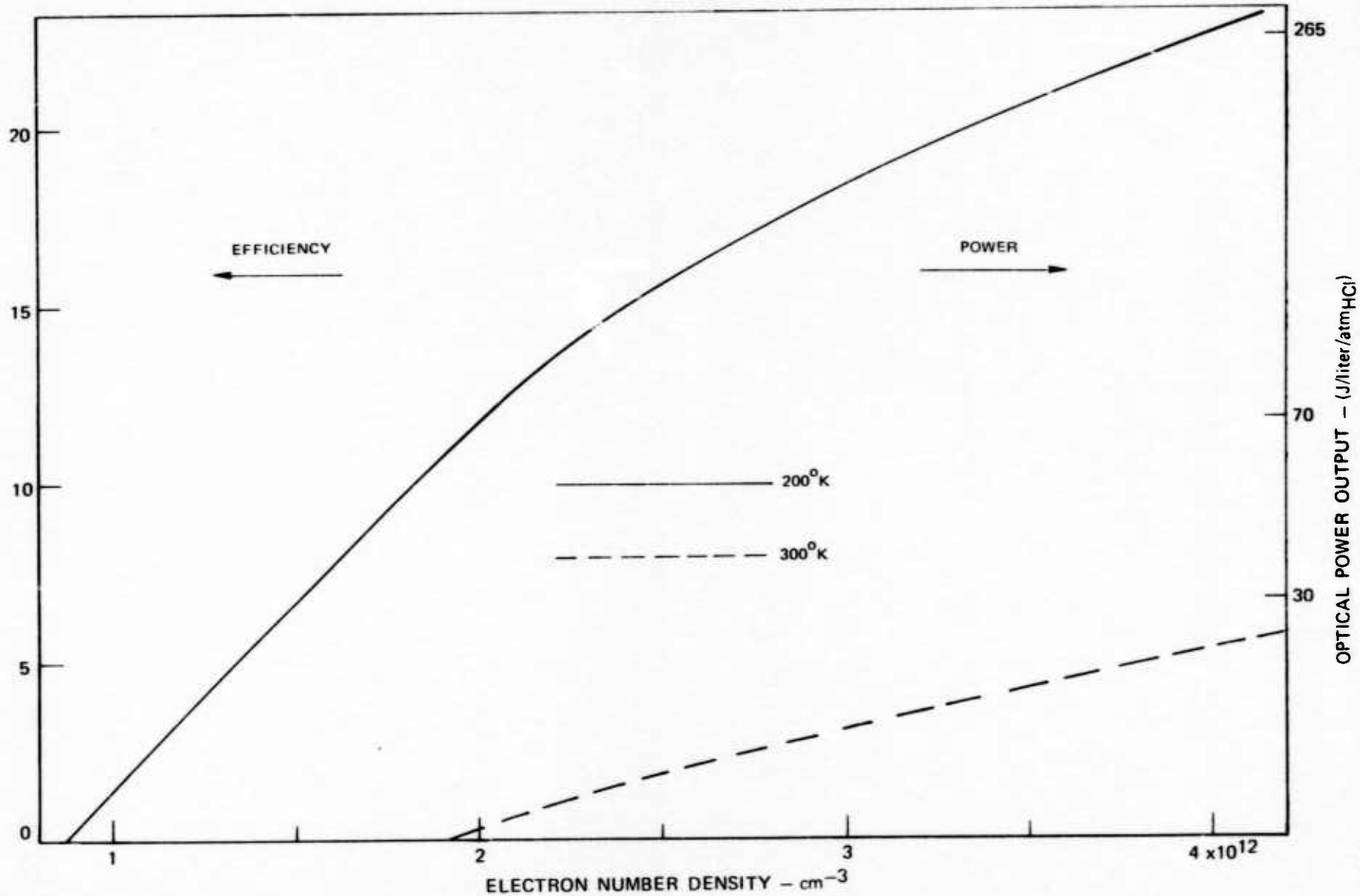

N06-205-1

N91340-13

FIG. 15

FIG. 16

CALCULATED SPECTRAL DISTRIBUTION OF HCl EDL OPTICAL POWER

HCl: H_e = 1:9

T = 200°K p = 10 torr

E/N = 1.25×10^{-16} V–cm^2

α_{CAV} = 2×10^{-4} cm^{-1}

– – – n_e = 2×10^{12} cm^{-3}

——— = 4×10^{12}

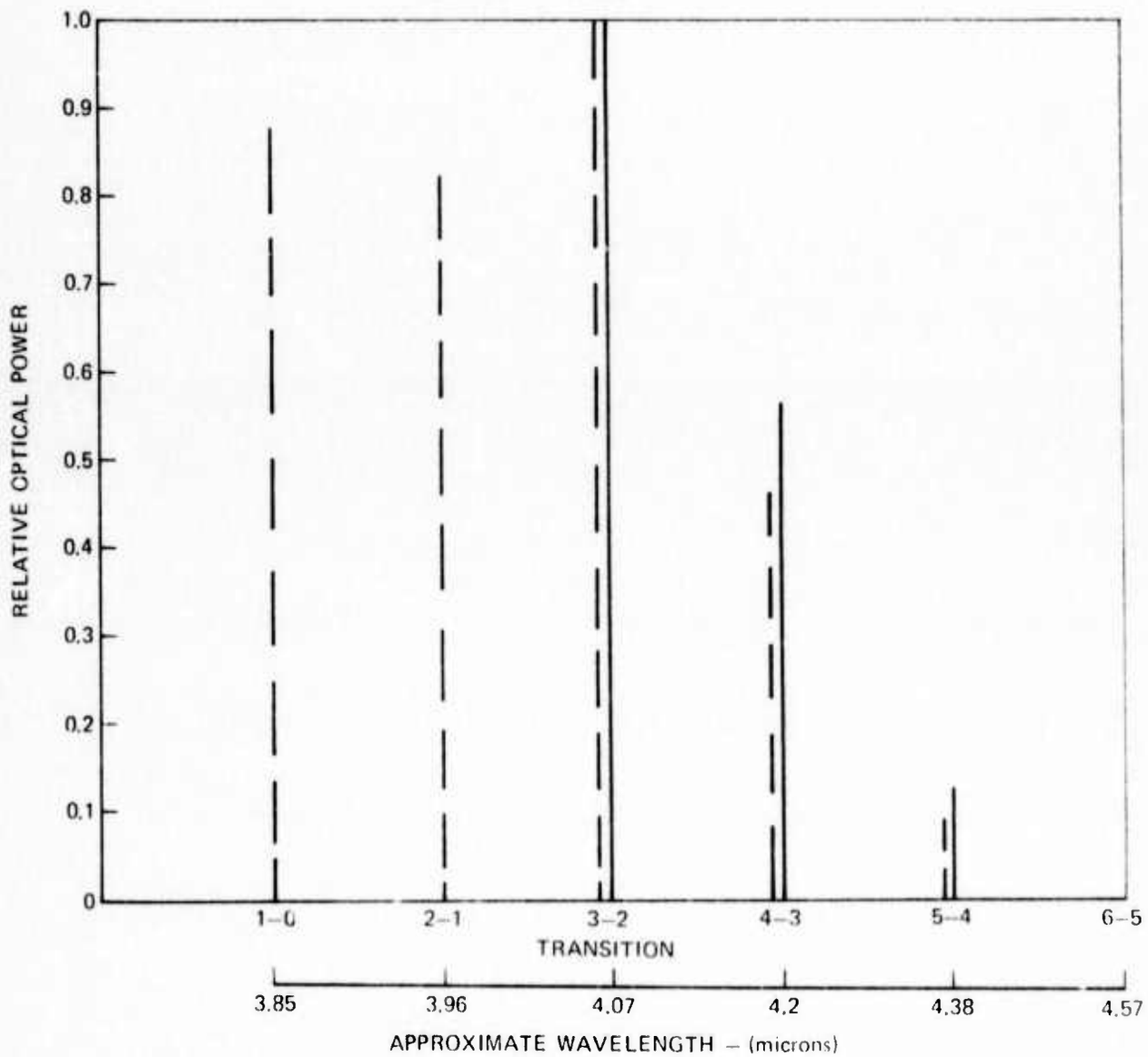

N06-200-1

IV. EXPERIMENTAL INVESTIGATIONS

The apparatus utilized to attempt to demonstrate electric discharge laser action on the vibrational transitions of HCl pumped purely by electric discharge is described in the first half of this section. The results of these experiments are described in the second part of this section.

The approach taken in this investigation has been to provide an auxilary source of ionization for the HCl electric discharge in order to attain a suitable range of stable operating conditions and sustain the relatively high electron number density required for development of population inversion.

Description of System

A photograph of the experimental apparatus is shown in Fig. 17. The individual components are described in detail in this section. Figures 18 and 19 show in schematic form the layout of the laser discharge tube and details of discharge circuits. An ionizing electron beam, average electron energy 180 keV, is propagated down a 2 in. I.D. discharge tube. A sustaining electric field is maintained in this tube by a high voltage pulsed power supply applied to electrodes at either end of the 96 cm length pyrex tube. The sustainer cathode, located near the electron gun, consists of a mesh of 0.012 in wires spaced 0.1 in apart in a rectangular pattern. This mesh is supported by an aluminum flange. Spaced 4 cm from this flange is another flange with a 1.9 in dia. hole. These flanges are connected electrically by external buss bars. Sandwiched between these flanges is a current transformer (Pearson Model 2100) which measures the beam current transmitted by the foil and the mesh. The anode is an aluminum flange with 19-0.25 in diameter holes to allow for the admission of the HCl/Ar mixture into the discharge tube. The sustainer pulser applies to the anode a square positive voltage pulse which is synchronized with the pulse applied to the electron gun. The resistor R_L limits the current in the event of an arc and R_G draws current through the output thyratron to maintain conduction (and hence voltage on the anode) when the discharge tube fails to breakdown. A high impedance, high voltage probe (Tektronix P6015) monitors anode voltage referenced to ground. Another current transformer (Pearson Mod. 411) at the anode connection monitors sustainer current.

A collimating magnetic field to aid e-beam propagation with minimum loss is maintained parallel to the discharge axis by a set of eight magnet coils arranged in a Helmholtz confriguration around the electron gun and discharge tube. The center line magnetic field is reasonably uniform decreasing somewhat at the ends of the array. Magnetic field intensity of 1000 gauss can be maintained in the central core, while the field diminishes to ~700 gauss at the foil holder.

The gas mixture flows continuously through the discharge tube entering at the anode and exiting through a 1 in. diameter sidearm 6 cm from the cathode. Gas flow rates are typically 2 liters/sec, so that the gas in the discharge volume is exchanged at a 1 Hz rate.

FIG. 17

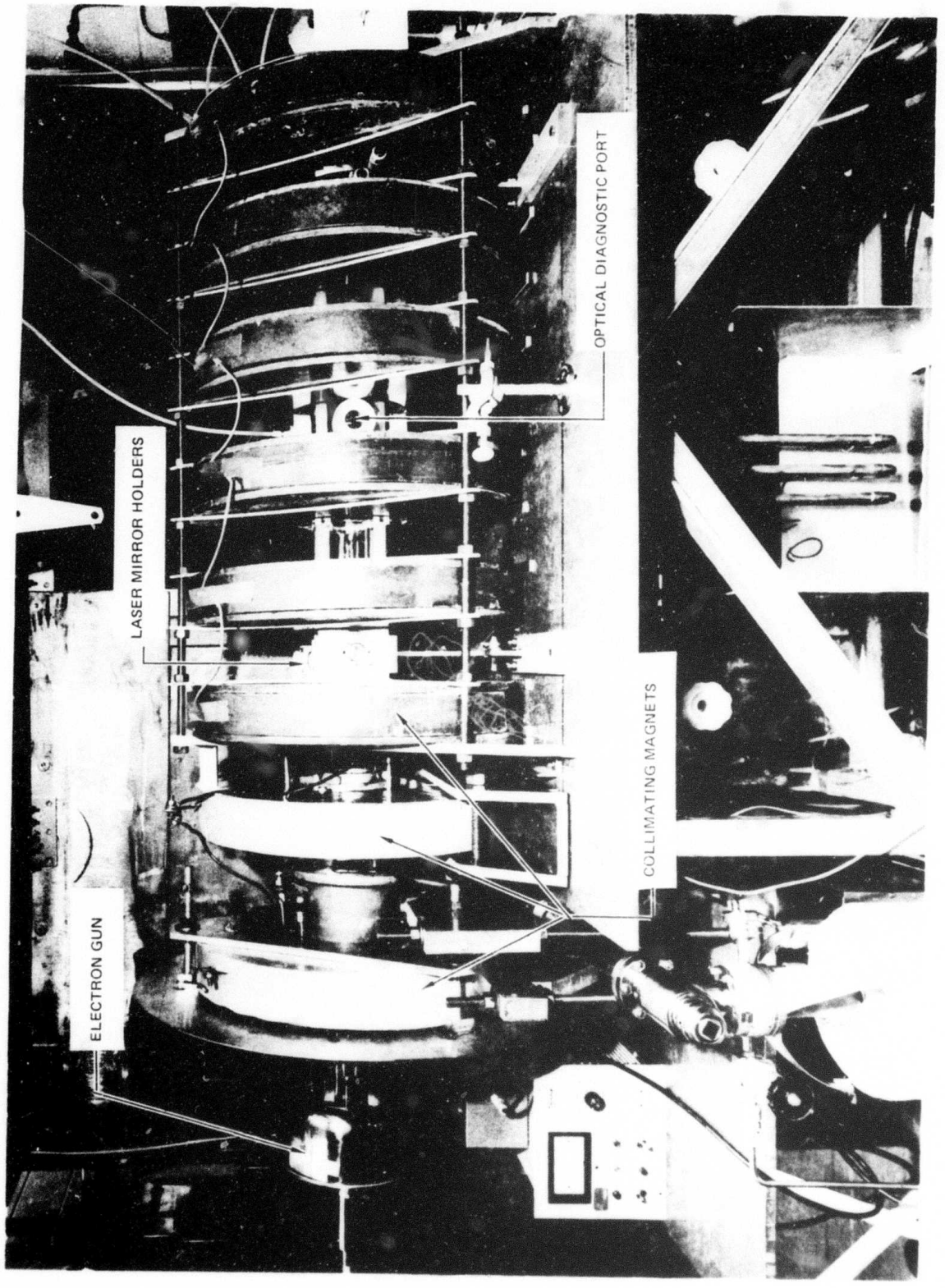
HCI PULSED ELECTRIC DISCHARGE EXPERIMENT
ELECTRON GUN
LASER MIRROR HOLDERS
OPTICAL DIAGNOSTIC PORT
COLLIMATING MAGNETS

FIG. 18

PULSED DISCHARGE LASER CONFIGURATION

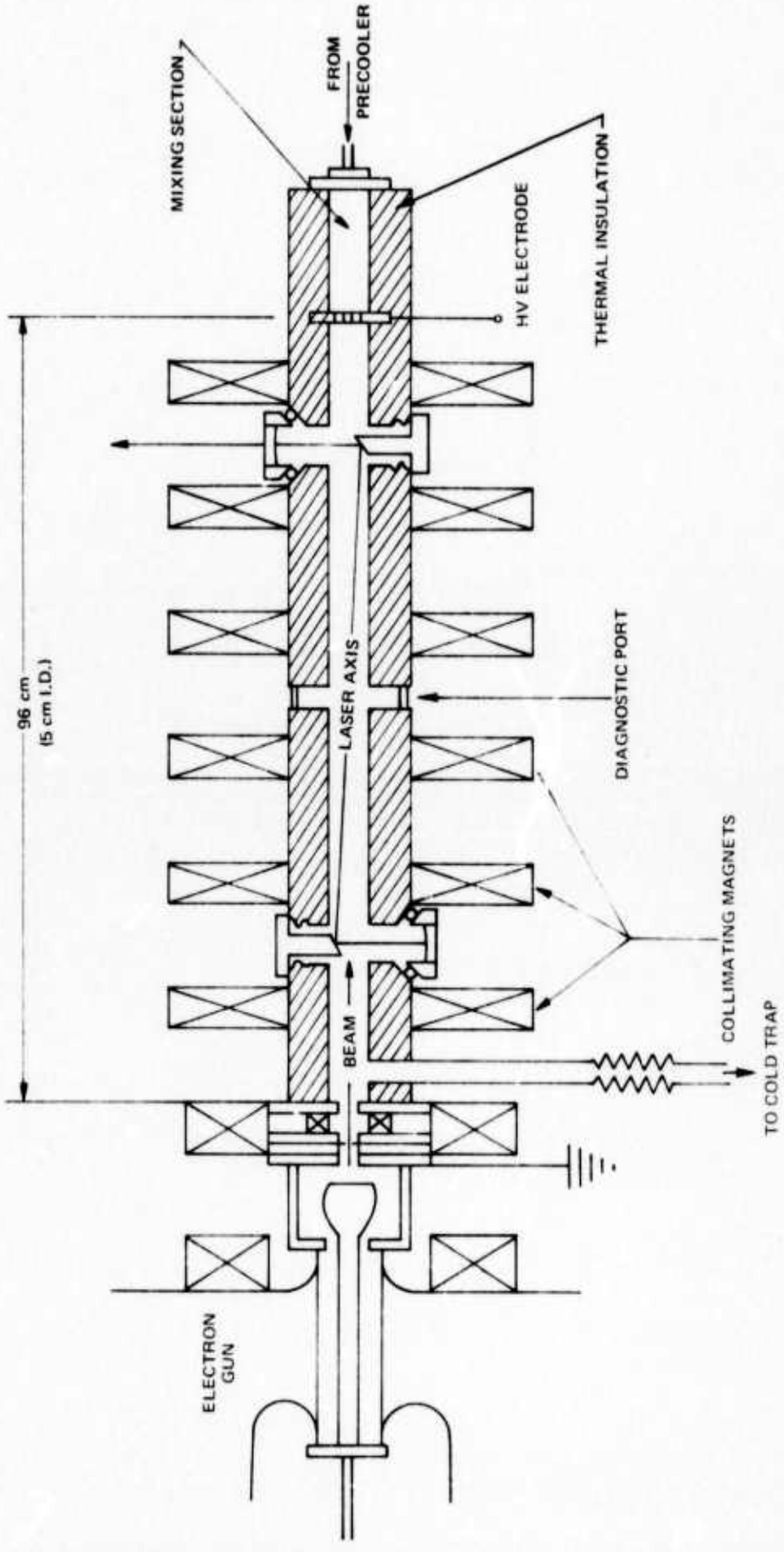

N08-21-7

FIG. 19

SCHEMATIC DIAGRAM OF DISCHARGE TESTS

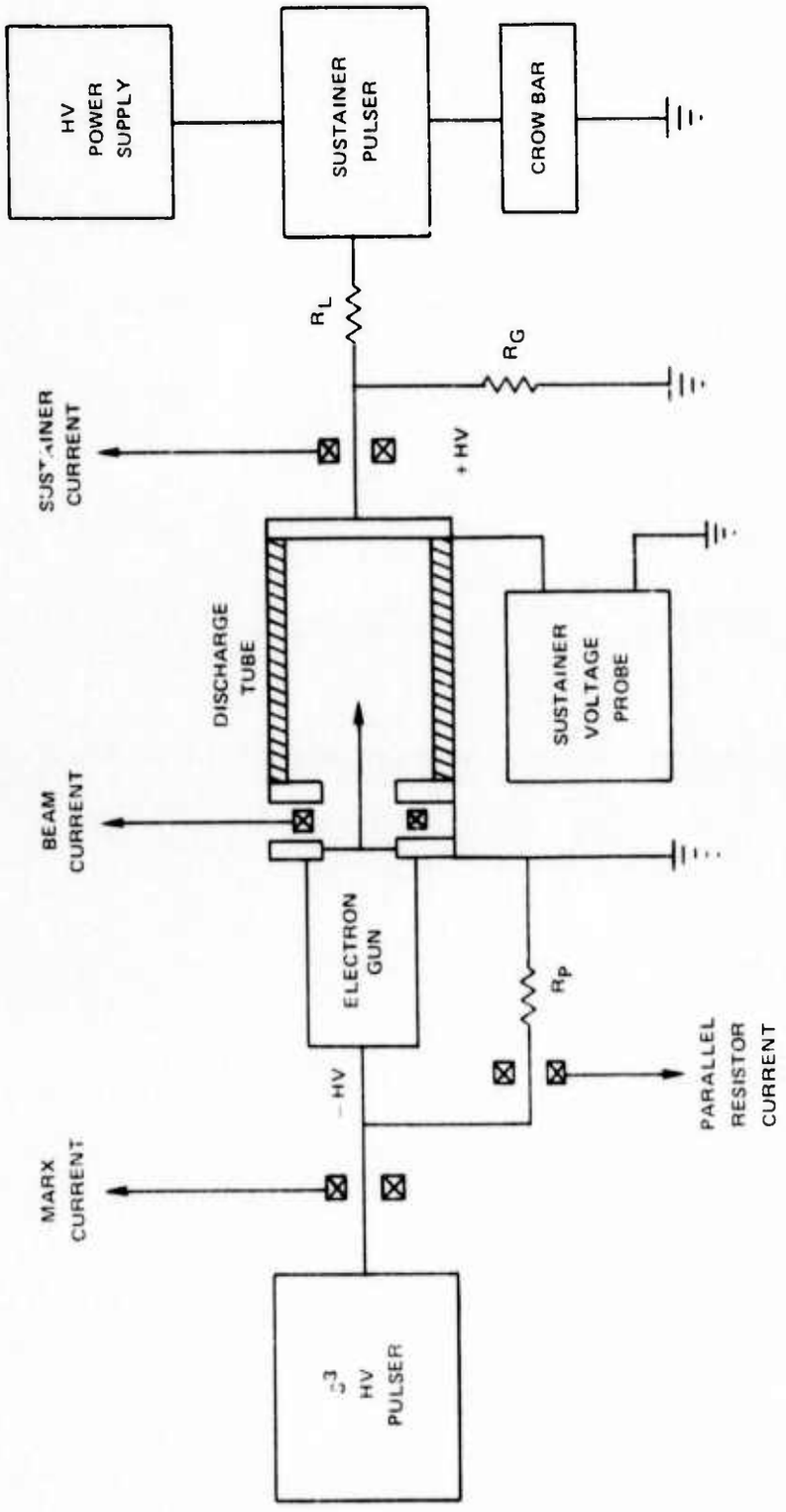

N05–144–1

Electron Beam System

The electron gun used in these experiments is a modified version of a high-voltage diode structure developed at UARL (Ref. 1). An external view of the UARL electron gun appears in Fig. 20. The gun basically is a close-spaced thermionic diode utilizing an indirectly-heated planar cathode. Extremely high fields (several times 10^5 V/cm) exist at the cathode surface. Consequently, current pulses are drawn in an emission-limited mode.

The cathode is a barium/barium oxide dispenser type (Phillips Metalonics) and has an emitting area of $\sim$3.14 cm^2. This cathode is capable of delivering over 100 A/cm^2 at 1630° K.

The foil support holder which was used in these experiments consists of a ½ inch polished plate with nineteen 0.25 inch diameter holes closely spaced in a hexagonal pattern. The foil which is typically 0.3 mil (20 micron) aluminum is sandwiched between this plate and another plate with a 1.4 inch diameter hole to allow maximum transmission of the beam.

The electron gun is energized by a high voltage (nominally 180 kV) pulse power supply designed and built by Systems, Science and Software (S^3) to UARL specifications (Ref. 24). Basically the pulser is a three-stage Marx bank with a pressurized, triggered spark gap used to terminate the high voltage pulse. The capacitance per stage (0.05 μf) is chosen so that the output voltage droop is $\lesssim$10 percent for a 110 microcoulomb pulse (11 amps for 10 μsec). Rise and fall times are less than 1 μsec. The S^3 unit can produce 5-20 μsec duration pulses of 180 kV at current levels from 5-20 amperes, at a rate of 1 pps. The output of the supply is delivered to the electron gun by means of a RG-300 coaxial cable. The connection to the electron gun is accomplished by ballasted grading rings used to minimize breakdown on the cable. A resistor, R_p, provides a load (drawing $\sim$5 amperes) when the electron gun is not emitting. Marx output current is measured by a shielded current transformer mounted within the Marx tank.

Optical Resonator

A stable resonator cavity has been installed on the discharge tube to provide a long optical path length in the longitudinal geometry. Figure 21 is a photograph showing the external skeleton of the stable cavity. Figure 18 illustrates schematically the optical path. Mirrors internal to the vacuum chamber are held in adjustable mirror mounts held in very short sidearms blown in the glass discharge tube. The mounts are o-ring sealed to the discharge tube. Two plane mirrors located opposite the end mirrors turn the optical axis so that the axis is skewed slightly with respect to the discharge tube axis. The turning mirrors are held at the end of pedestals near the outer edge of the discharge tube, so as to impose as little disturbance to the discharge as possible. These pedestals are mounted in coarse mirror mounts to allow for adjustment of the internal mirrors. The internal turning mirrors are separated by 61 cm. The active optical core is estimated to be approximately 56 cm. The end mirror/internal mirror holder assemblies are held stably by

FIG. 20

UARL THERMIONIC DIODE ELECTRON GUN

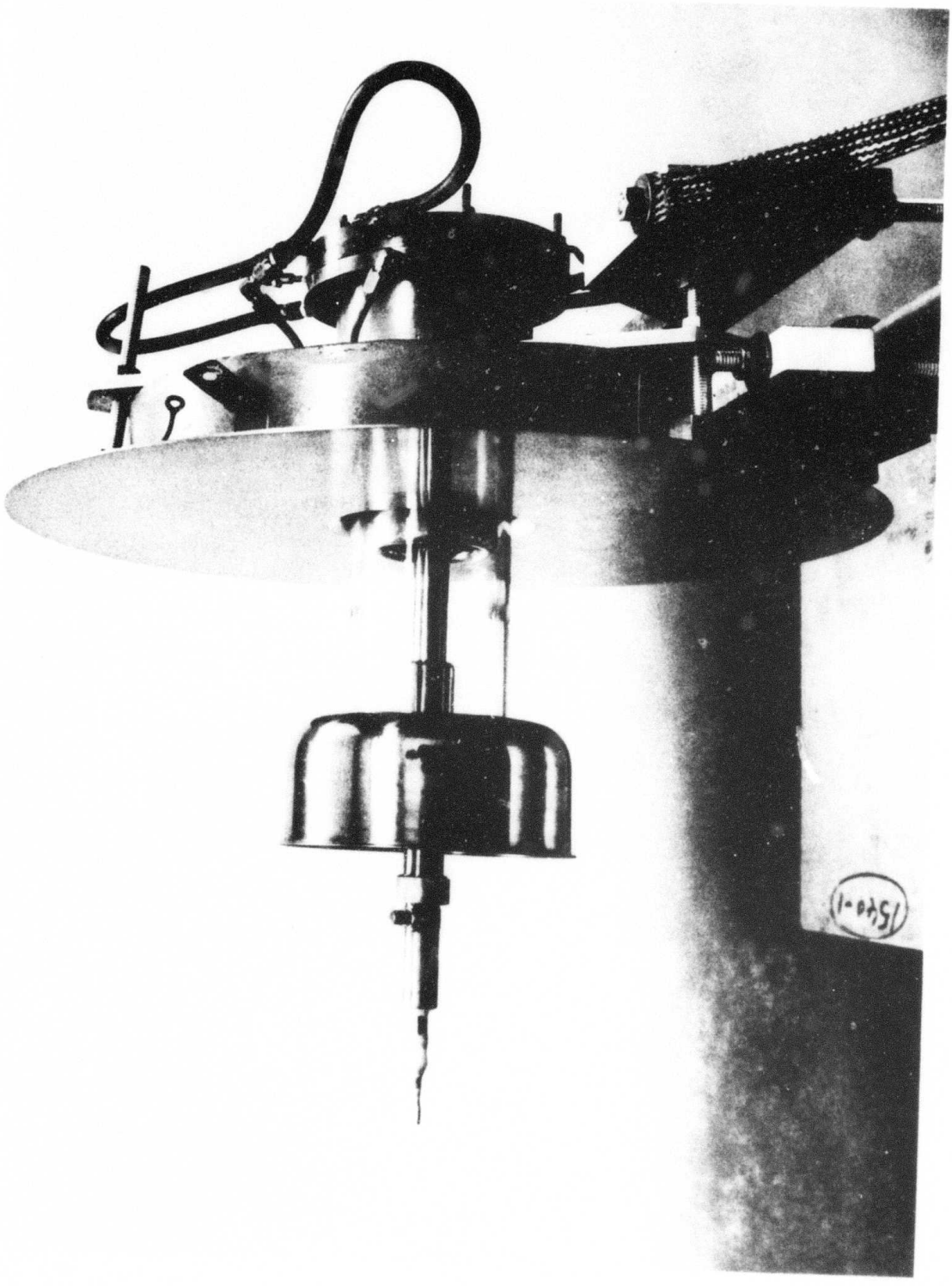

FIG. 21

STABLE OPTICAL RESONATOR

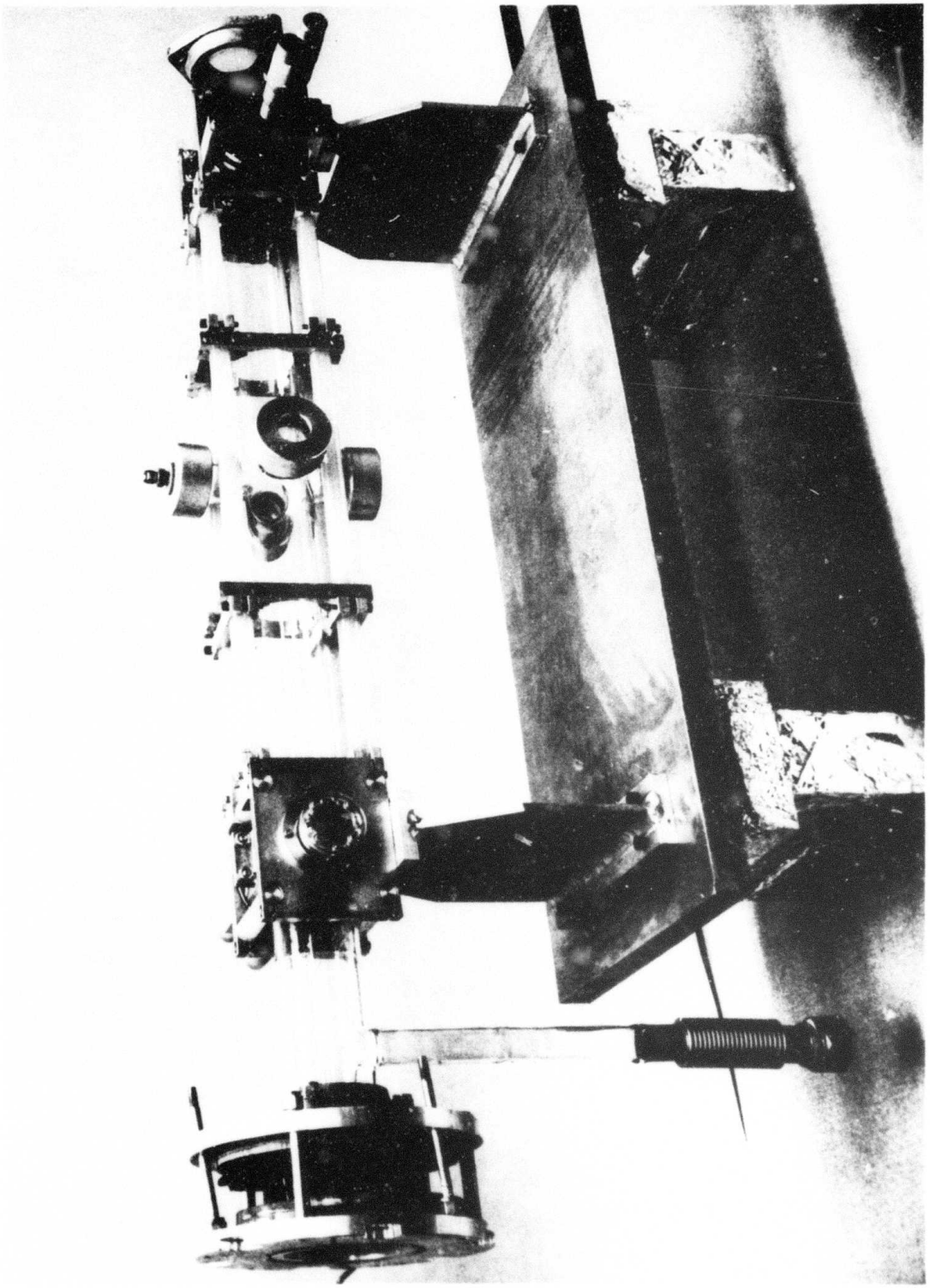

Cer-vit (Owens-Illinois) rods separating the two holders (see Fig. 21). The two mirror assemblies at either end of the discharge tube are separated by additional Cer-vit rods, so that the mirrors are held to the discharge tube independent of the thermal fluctuations of the discharge tube.

Two sets of optics have been used in these experiments. One set is gold coated and hole coupled. The two internal mirrors are 0.50 inch diameter fused silica flats. One end mirror is 1.0 inch diameter and has a radius-of-curvature of 2 m. The others is also 1 inch diameter but has a 2 mm hole and a 10 m radius of curvature. The coupling hole is vacuum sealed by a Irtran 2 flat epoxy bonded over the hole. The other set of optics has silicon substrates. The two internal mirrors are 19 mm diameter and 3 mm thick flats. They are coated for maximum reflectivity with thorium fluoride enhanced silver. The two end mirrors are 25 mm diameter and have a radius-of-curvature of 2 m. One mirror is dielectric coated for maximum reflectivity ($r \gtrsim 99.7\%$ spec.). The output mirror is coated for $r \sim 99.5\%$ and the back surface is anti-reflection coated.

Gas Handling

A flow diagram of the gas handling system is shown in Fig. 22. Argon and hydrogen chloride are regulated and metered through flow meters. The gases flow separately to the discharge apparatus where they are mixed at low pressure in a glass tube attached to the anode. The argon stream can be cooled by a copper coil immersed in liquid nitrogen. After flowing through the discharge tube the gases exit by means of a sidearm near the foil holder. The gases then are conducted through a copper liquid nitrogen cooled cold trap, where HCl is effectively removed from the gas stream. Bellows sealed cryrogenic valves are used to isolate this trap. After an experiment the contents of this trap are neutralized by bubbling through a column filled with NaOH solution.

The argon used is supplied in prepurified form. The hydrogen chloride is electronic grade and is used without further purification except for flowing through a molecular sieve trap.

The discharge tube pressure is measured with an absolute pressure gauge (Wallace-Tiernan) connected to a sidearm in the center of the discharge tube. Thermocouples at the entrance and exit of the discharge tube are used to measure temperatures. The discharge is insulated with two inches of closed cell styrofoam in bead form. With this the lowest temperatures attainable are $\sim 150^\circ$K at the discharge inlet. At these conditions the exit temperature is approximately 90°K higher.

Emission diagnostics

Located in the center of the discharge tube is a cross with one part of the cross sealed with a sapphire window. Spontaneous emission originating from the center of the discharge tube is imaged by a CaF_2 lens (1.5 in diameter 5 in focal length) into a cooled InSb detector. An uncooled wideband pass

GAS HANDLING SYSTEM

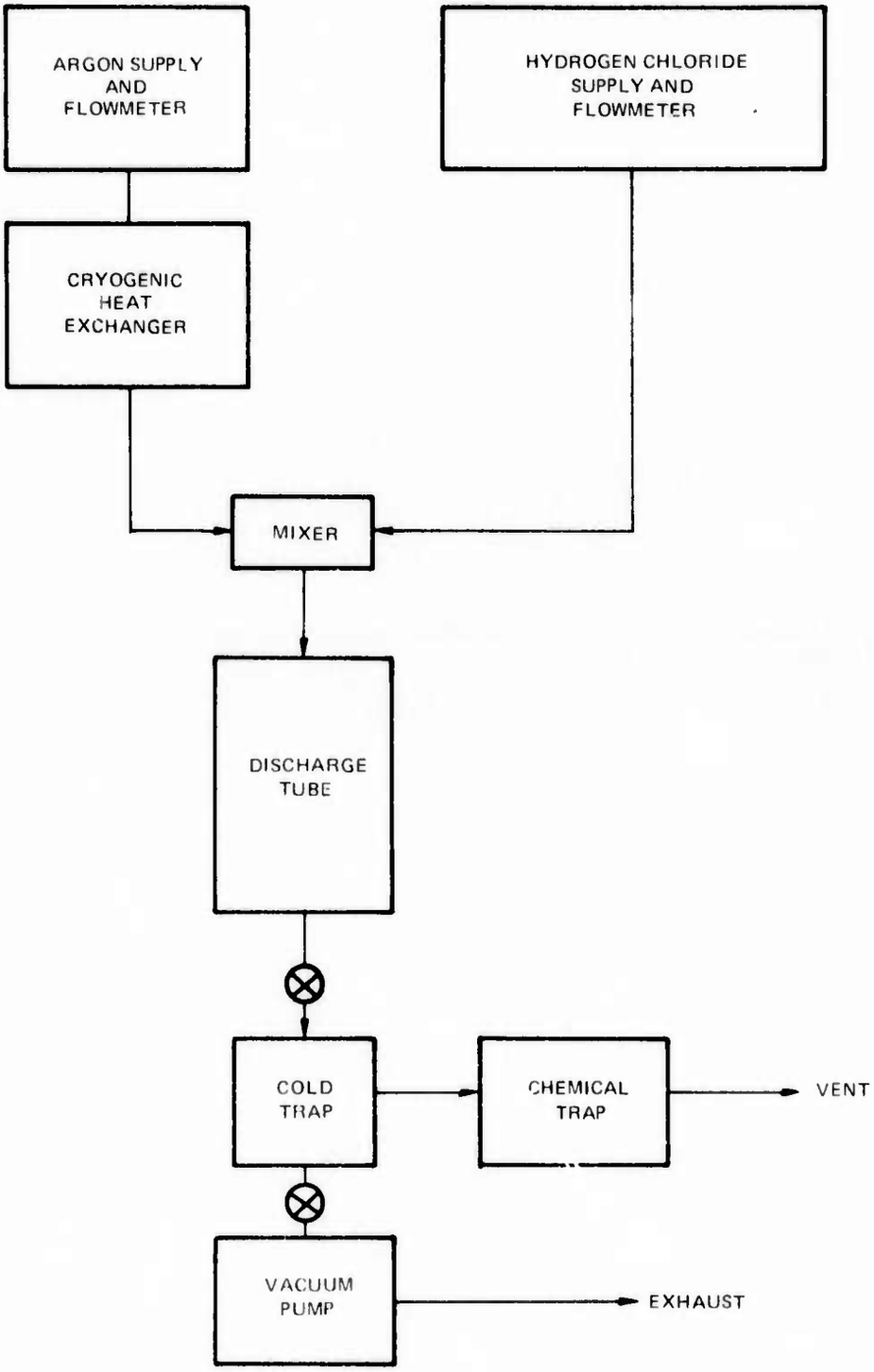

N08-21-5

filter ($3 \leq \lambda \leq 4.2\mu$) is positioned just in front of this detector. Another detector (liquid N_2-cooled Ge:Au) filter combination is located coincident with the laser output axis. Both of these detectors and associated oscilloscopes are located in a screen room next to the table supporting the experiment. Both detectors are additionally enclosed in RFI tight boxes with a small hole allowing for beam entrance. Additional signals from current and voltage probes are brought into the screen room with coaxial cables. The outer shield of these cables is connected to the outer screen of the double wall screen room. These precautions were not sufficient to eliminate noise in the detector circuits however the remaining noise was confined to disturbing only the leading edge of the anticipated signals.

Experimental Results

Beam Transmission Tests

Of critical importance to the maintainance of stable high conductivity hydrogen chloride doped discharges is the source of ionization, in this case the ionizing collisions between primary electrons and the background gas.

The "range" of electrons, L, in the background gas can be estimated from the expression (Ref. 25)

$$L = \frac{1}{V_i} \int_o^V \frac{dv}{\beta s(V)}$$

where V_i is the ionization potential of the gas, β is the ratio or the average energy lost per ionizing collision to the ionization energy, $s(V) = n_{go} Q_i$ is the ionization mean free path, Q_i is the ionization cross section and n_{go} is the gas number density at standard conditions (room temperature, 1 Torr). For the electron energies of interest here the reduced ionization mean free path in argon can be approximated by a simple exponential expression (Ref. 25):

$$s(V) = C\, V^b$$

and

$$C \approx 680$$

$$b \approx 0.766 \quad .$$

The average energy lost per ionizing collision for argon has been found to be 26.2 eV (Ref. 26), thus $\beta \approx 1.67$. The electron range in argon has been calculated from this simplified expression and is shown in Fig. 23, for several reduced pressures, $p = p\frac{T_o}{T}$, where p is discharge pressure and T and T_o are discharge and reference (293°K) temperatures respectively.

It is clear from this figure that in the present experiments, which are conducted at relatively low pressure, (p=10-20 Torr) high initial electron energy is not necessary from range considerations. However it will be shown that high electron energies are required from foil transmission considerations. In the range calculation the initial electron energy is the average electron energy after passing through the foil.

FIG. 23

ELECTRON RANGE IN PURE ARGON

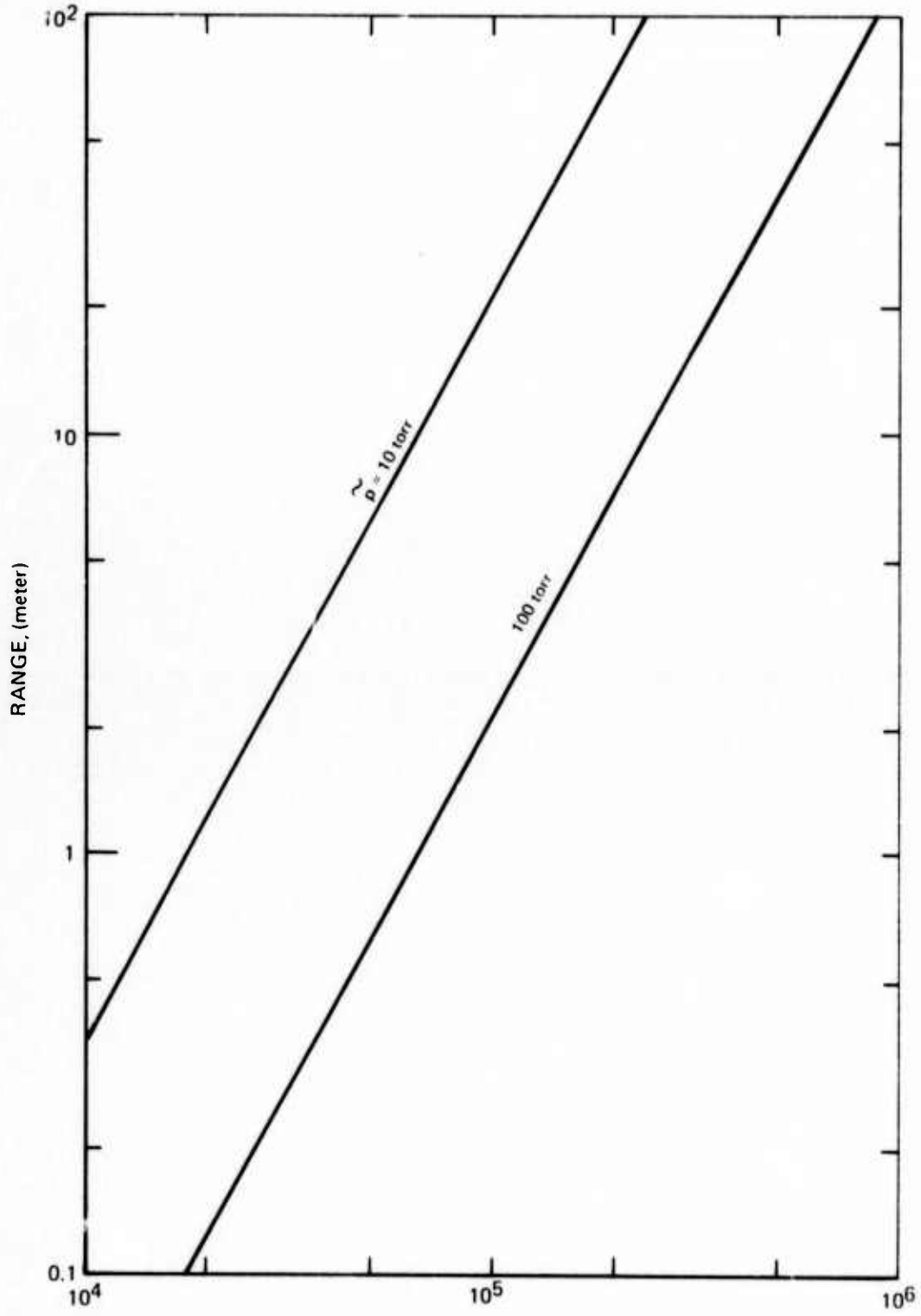

N08-21-9

The electrons emitted from the thermionic cathode are essentially monoenergetic at the anode plane. On passing through the foil, the electrons typically suffer many collisions and the emergent beam is degraded by absorption, scattering and energy loss. The transmission Ψ of the foil is given by the ratio of emergent to incident current:

$$\Psi = \frac{i_1}{i_o} \quad .$$

The ratio of the average residual energy to the incident energy is

$$F = \frac{\bar{U}_1}{U_o} \quad .$$

Ψ and F can be evaluated from excellent expressions availabe in the literature (Ref. 27). These quantities are shown as a function of incident energy in Fig. 24 for 0.8 mil aluminum foil.

The instantaneous power absorbed in the foil per unit area can be shown to be

$$P_f = j_G U_o (1-\Psi F)$$

where j_G is the incident electron current density. The energy absorbed in the foil in a single pulse then is

$$\epsilon_f = \int_o^t j_G U_o (1-\Psi F) dt \quad .$$

This expression has been evaluated for conditions typical of these experiments. These results are shown in Fig. 25 as a function of j_G for a nominal 10 microsecond pulse. Also shown is the energy corresponding to foil melting. It is expected that the foil will fail mechanically due to exceeding the ultimate stress at elevated temperature. The incident current density should be limited to $\sim$10 A/cm^2.

The foil also represents a scattering source suffering some electrons to exhibit large angular deviations from the incident direction. In Fig. 26 the fraction of electrons contained within various cone half angles are shown as a function of beam energy for an 0.8 mil aluminum foil (ref. 28). It is seen that even at 180 keV a sizable portion of the beam emerges with angular deviations in excess of 40 degrees. Scattering represents a potential source of loss since electrons scattered in angles larger than 1.5 degrees will encounter the walls of the relatively high aspect ratio ($\approx$20) discharge tube.

The collimating magnetic field serves to counter-balance the effect of scattering. A scattered electron has some motion perpendicular to the discharge axis which is characterized by an energy U_1. The magnetic field converts the

FIG. 24

TRANSMISSION AND RESIDUAL ENERGY OF ELECTRONS INCIDENT ON 0.8 MIL ALUMINUM

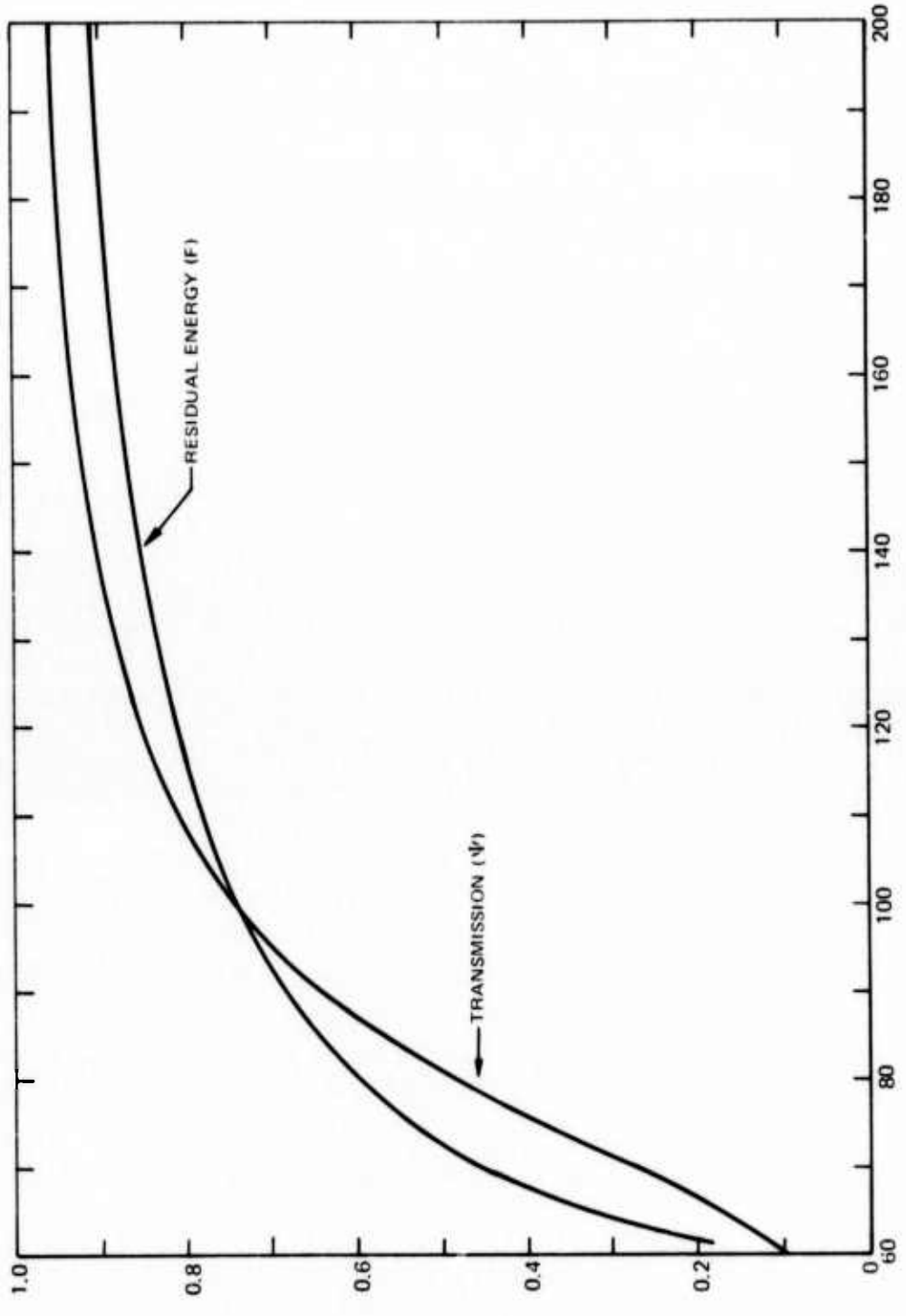

N08-21-8

ENERGY DEPOSITION IN 0.8 MIL ALUMINUM FOIL

U_o = 180 kV
τ_p = 10 μsec
C = 0.03 μf
$\tau_{RISE} = \tau_{FALL}$ = 1 μsec

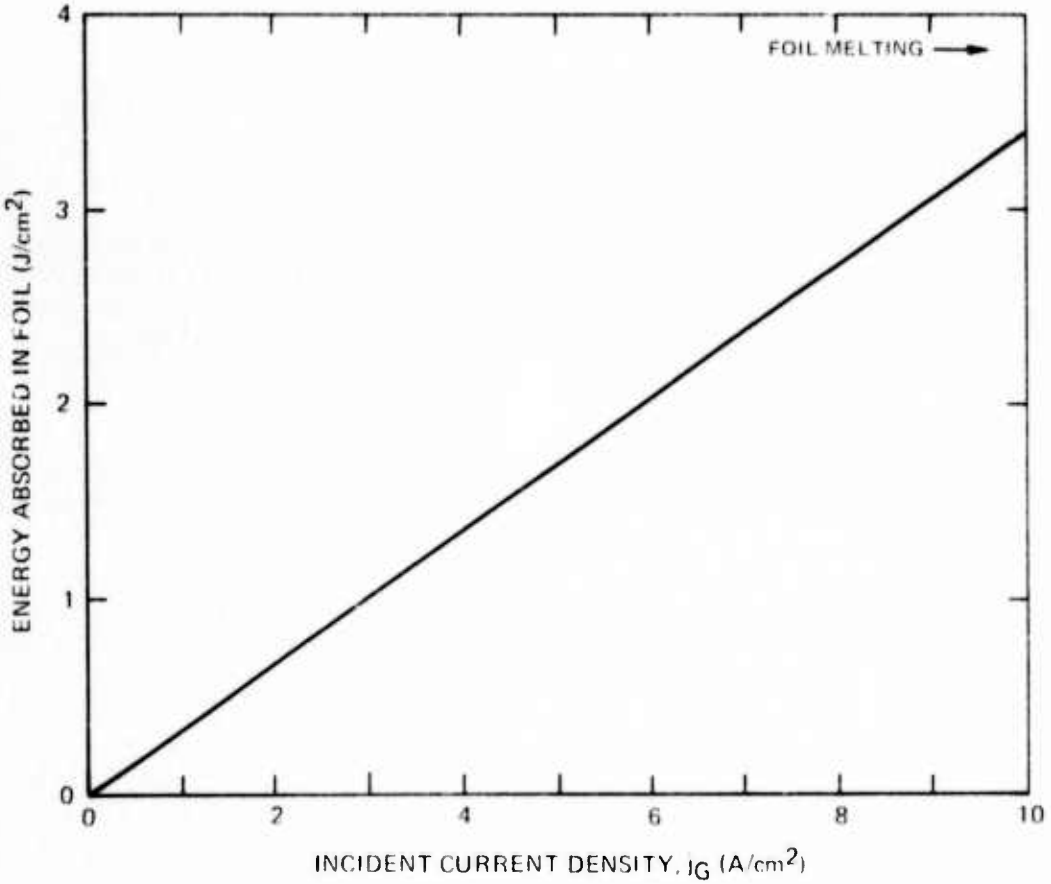

ANGULAR DISTRIBUTION OF TRANSMITTED ELECTRON BEAM

(WITHOUT MAGNETIC FIELD)

0.8 MIL ALUMINUM FOIL

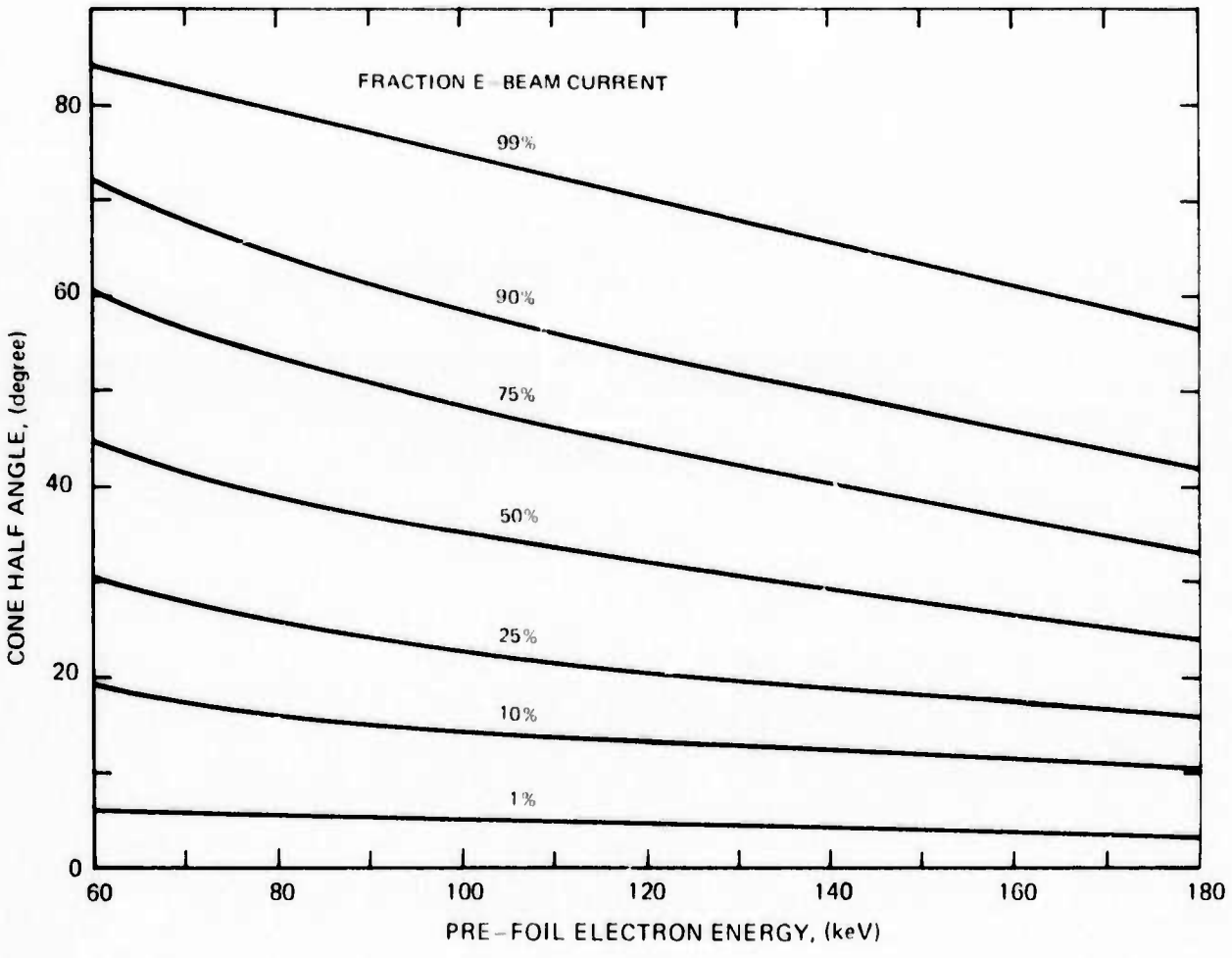

N08-21-2

perpendicular motion into a rotary motion, so that in the absence of collisions the electrons orbit down the magnetic field lines. The radius of the electron orbits is given by the classical formula for the cyclotron radius, r:

$$r = \frac{1}{B}\sqrt{\frac{2m_e U_1}{e}} \quad ,$$

where B is the magnetic field strength, m_e is the electron mass, and e is the electronic charge. The fraction of electrons with orbital radii less than R is shown in Fig. 27 for several values of magnetic field strength. Incident energy of 170 keV is assumed for this figure, this value be typical of the temporally average electron energy.

The effective transmission of the electron gun firing into argon/hydrogen chloride has been measured by comparing the current incident of the foil (obtained from the Marx bank current transformer subtracting the current through the parallel resistors) with the current measured by the beam current transformer when the sustainer field is off. These quantities are plotted against one another in Fig 28. Although there is considerable scatter in the data, most points lie between

$$12 \lesssim \frac{I_g}{I_b} \lesssim 30.$$

The half angle of the cone subtended by the discharge wall at the current probe is 20 degrees. Variation of the collimating magnetic field had little effect on the transmission, it did have a pronounced affect on the sustainer discharge as will be discussed below.

Discharge Tests

Experiments have been performed with a hydrogen chloride/argon discharge sustained by the UARL electron gun. An example of the experimental data obtained is shown in Fig. 29. This figure is taken directly from tracings of oscilloscope photos. Three signals--sustainer voltage, V_s beam current, I_B, and sustainer current, I_s--were displayed on a Tektronix 7403 scope with chopping plug-ins, thus the beam appears as dotted line segments. The uppermost trace labeled I_B and the lower three traces were taken on successive shots at the same filament heater power. On the uppermost trace the sustainer field was turned off. The lower three traces are of a single discharge with the sustainer field turned on. It will be noticed that the current measured by the beam probe is not the same on both photographs. The discrepency is accounted for by the fact that when the sustainer field is on a portion of the sustainer current is drawn through the beam probe as it is in the sustainer field. For this reason true beam current is measured with the sustainer field off as in the uppermost trace. It has been found that once the cathode temperature is stabilized there is little difference in measured true beam current from shot to shot.

FIG. 27

FRACTION OF BEAM WITH GYRO RADIUS LESS THAN R_L

U_o = 170 keV

0.8 MIL AL

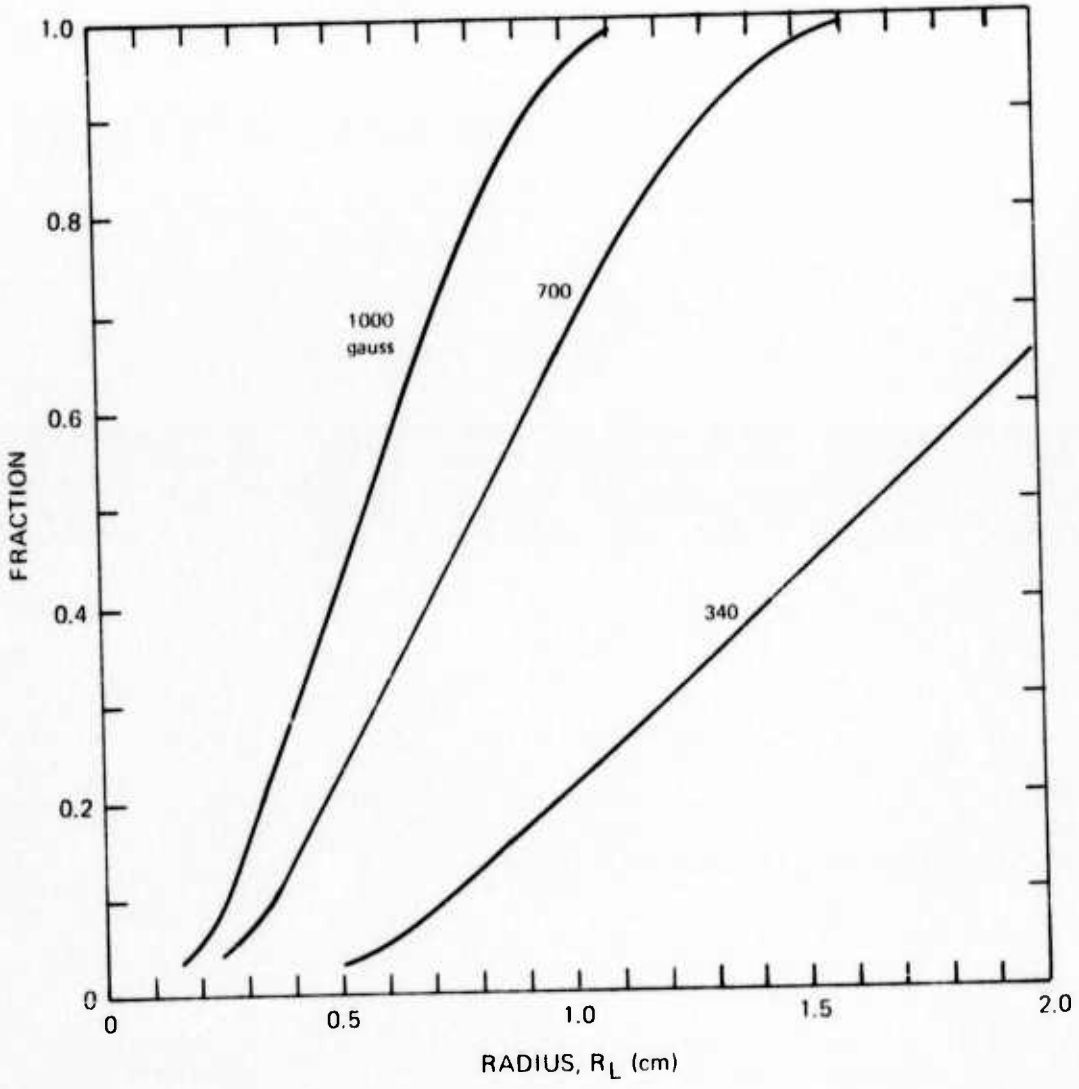

N08-21-3

FIG. 28

EXPERIMENTAL ELECTRON TRANSMISSION

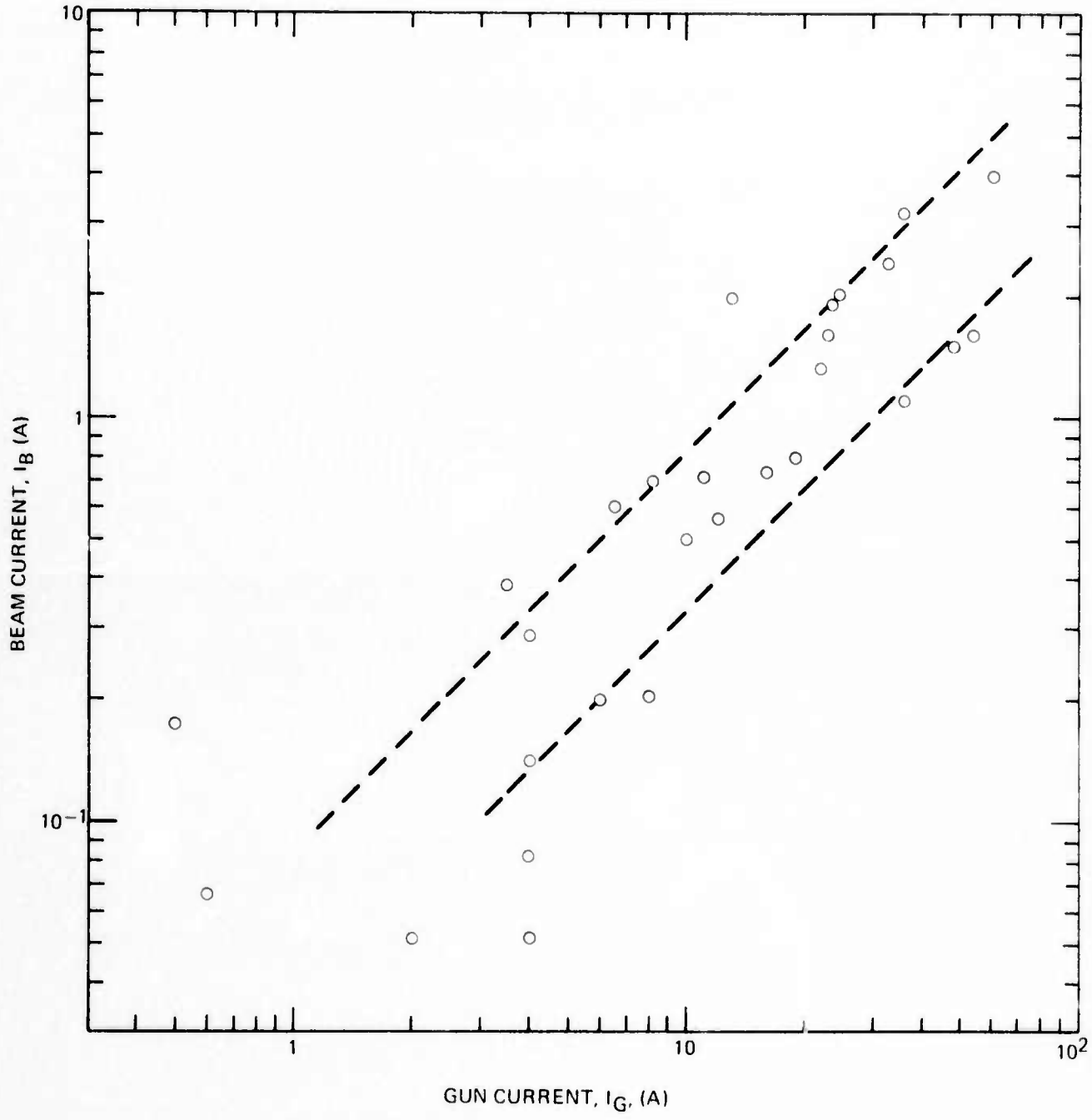

N08-21-4

HCl/Ar DISCHARGE DATA

(TRACED FROM OSCILLOSCOPE PHOTOS)

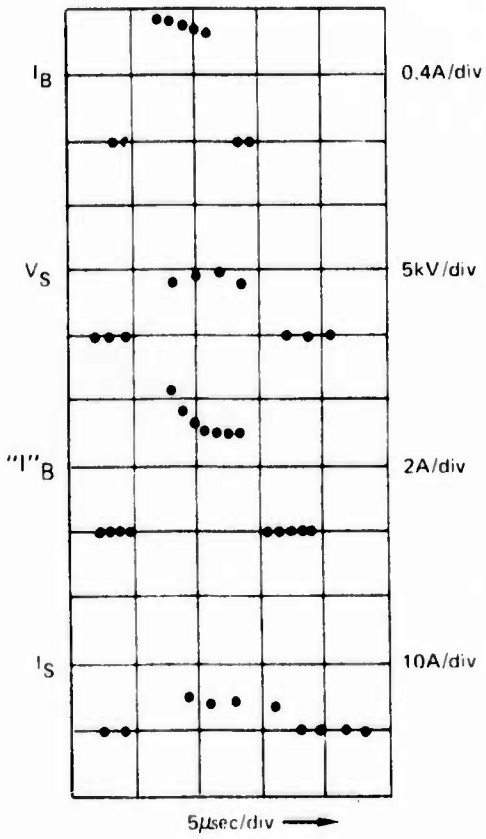

The results of several experimental runs are shown in Fig. 30. In all cases the discharge was initially at room temperature and the total pressure was 10 Torr with 5% HCl/95% Ar mixture. This figure shows the electron number density as a function of e-beam current density, j_B (j_B is obtained from the measured beam current divided by an area typical of the beam at the beam probe--i.e. $5cm^2$). The electron number density n_e, was obtained from the current balance

$$j_S = \frac{I_s}{A} = en_e v_d,$$

so that

$$n_e = \frac{I_s}{ev_d A} \quad ,$$

where j_s is the sustainer current density, I_s is the measured sustainer current, A is the discharge area (assumed equal to the discharge tube cross sectional area), e is the electronic charge. Values of electron drift velocity, v_d, have been taken from Fig. 31, which plots this variable versus E/N for two HCl/Ar mixtures. An indication of the average value of electron energy, ϵ_k, has been also presented. These curves have been calculated numerically from the Boltzmann equation using the cross sections for the various pertinent processes which have been reported (Ref. 2). These calculations are probably valid within a range of ±5%.

The data presented in Fig. 30 follow a $n_e \sim J_b^2$ dependence as is shown by the line drawn. It was previously reported that the data indicated $n_e \sim J_b$, which dependency was found subsequently to be incorrect as more data were acquired. As a result of a leak in the cold trap, the mixture in the original run had not been carefully controlled and in fact was not precisely known, hence these points have been omitted from Fig. 30.

Also shown in Fig. 30 is a pair of points with the magnetic field turned off. At the higher beam current density, the lack of a collimating field has a pronounced effect, decreasing the ionization yield by a factor of one-fourth.

As has been indicated previously, it was expected that the discharges would be controlled by dissociative attachment in hydrogen chloride. This mechanism would yield a $n_e \sim J_b$ dependence. The recombination mechanism dominating the discharge is not known. The usually dominant dissociative recombination mechanism in pure argon at these pressures is much slower (Ref. 29 and 30) than the calculated rate of dissociative attachment in HCl. It is possible that electron-ion recombination in HCl is dominant. Further work is needed to elucidate the operative mechanism.

Spontaneous and Stimulated Emission Tests

Due to the considerable difficulties experienced in developing reliable repetitive operation of the high voltage pulser for the electron gun, actual experimental activity was severely limited. The series of tests searching for HCl laser emission in this apparatus was limited to only 6 individual experiments.

FIG. 30

ELECTRON NUMBER DENSITY IN HCl/Ar MIXTURE AS A FUNCTION OF E–BEAM CURRENT DENSITY

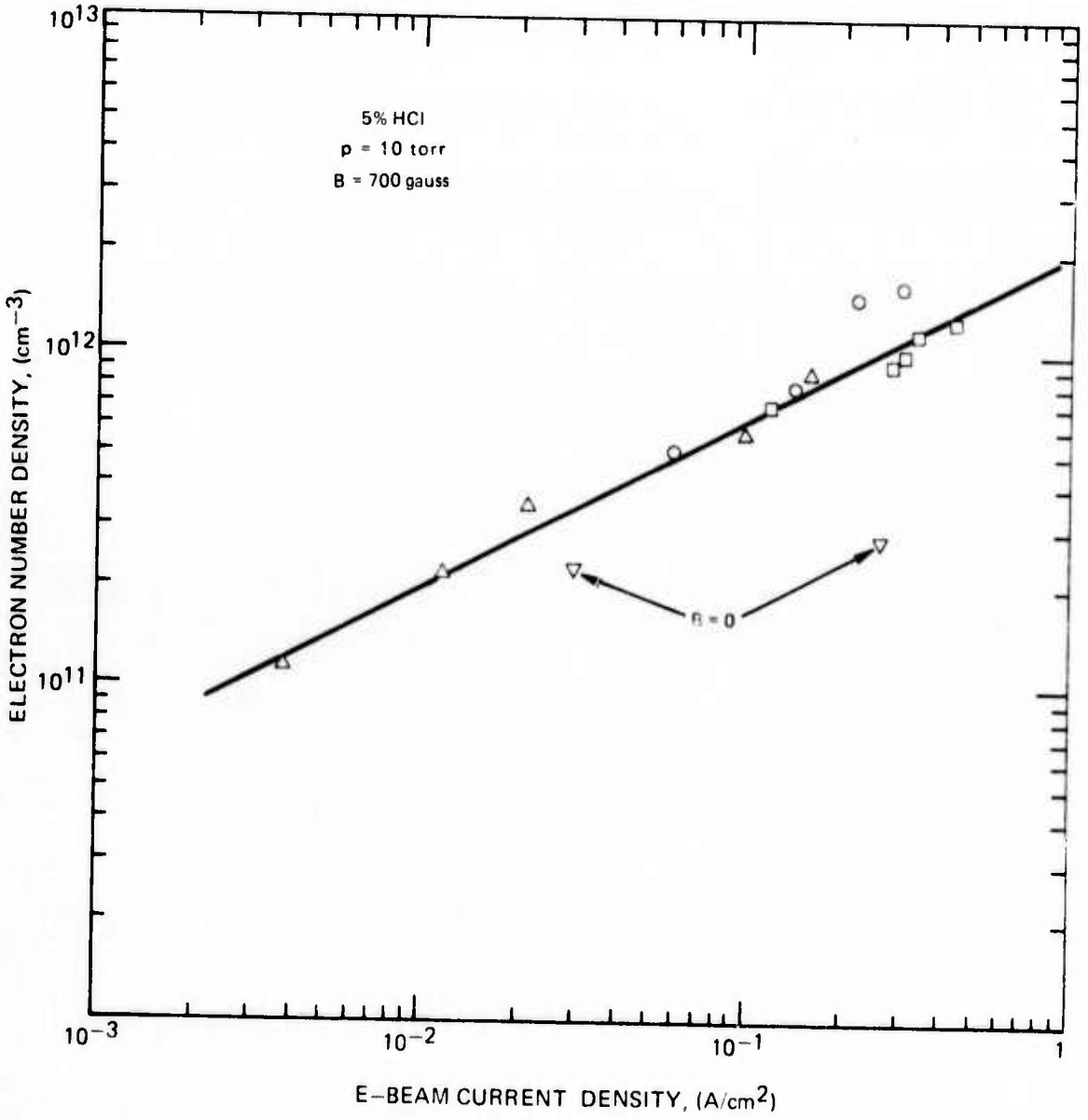

NO8 21-6

FIG. 31

ELECTRON DRIFT VELOCITY IN HCl/Ar MIXTURES

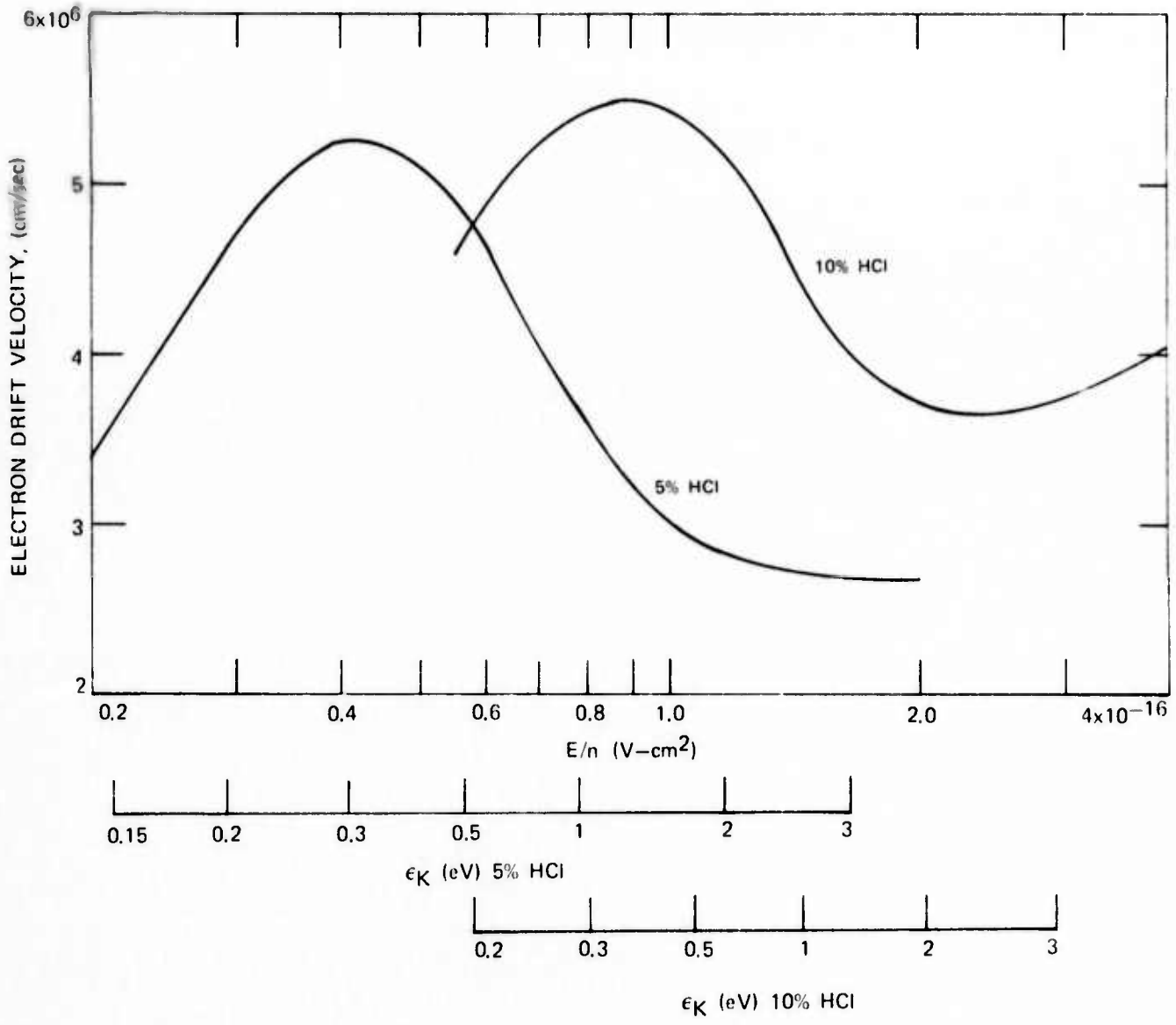

N05-172-2

In a series of tests, attempts were made to observe spontaneous and stimulated emission from the cavity nominally at room temperature. In all these tests the electron number density was below 1.6×10^{12} cm^{-3}. These tests were unsuccessful with no unambiguous evidence for laser action or spontaneous emission being observed. Both sets of optics previously described were utilized. The laser mirrors were aligned with a He-Ne laser at either end of the optical cavity. The optical axis was first established by aligning the coincident laser beams on the centers of the two interval mirrors. These mirrors were lined up by centering the beam, reflected from these mirrors, on the end mirrors. Then the end mirrors were individually placed in position, aligned and the position of the beam reflected off the back sufrace of the mirror was noted if it wasn't coincident with the incident beam. Both mirrors were then placed in position and the system was evacuated. The end mirrors were then realigned if they shifted. The internal mirrors were found not to shift under vacuum loading, the reason being that these mirrors are bellows sealed with four opposing adjustment screws. With these screws locked the mirrors do not shift. The end mirrors are O-ring sealed and a small shift under vacuum loading was noticed on one of the mirrors.

Considerable difficulties were encountered in conducting the emission tests. Noise generated by the Marx bank interfered with spontaneous emission detector. Noise levels, even inside the screenroom, were sufficient to saturate the detector preamplifier, which required several milliseconds to recover. This problem was finally overcome by locating both the detector (Raytheon Model - DN-1(s) InSb), and a preamplifier (Perry Amplifier Model 720) within a single heavy-wall copper enclosure. In addition to the noise difficulties, premature failures of the beam foil were encountered. This problem in most cases was due to an inadequate cathode activation resulting in non-uniform electron impact on the foil. This e-beam non-uniformity resulted in locally high heating rates and attendant foil failures.

In one case a short spontaneous emission pulse was observed when the wide-band pass filter was removed. Replacement of the filter eliminated the signal. The source of this emission has not been identified. It is likely originated from spontaneous emission from electronic states of argon.

The theoretical calculations indicate that with the electron number density attainable (i.e. $\sim 1.5 \times 10^{12} cm^{-3}$) laser threshold is not likely to be achieved at 300° K; an experiment was undertaken ultilizing the argon precooler to chill the discharge to 200° K average temperature. This test was terminated when the beam current level was found to be inadequate due to the failure to remove a piece of protective tape covering the foil holder. A further difficulty was revealed in this test. It was found upon examination that the coating on the upstream internal mirror had de-laminated. This defect was probably caused by unequal thermal contraction between the silicon substrate and silver coating. The temperature in the neighborhood of this mirror can reach 150° K. The other mirrors were unaffected.

V. CONCLUSIONS

Conclusions

On the basis of the investigation described in this report several conclusions can be drawn. The theoretical analysis of the HCl electric discharge pulse laser indicate that:

(1) Efficient laser operation requires $n_e\tau \geq 2 \times 10^7 cm^{-3} sec^{-1}$. It is understood that there is a limit to the useful excitation pulse length, τ, in that the pulse duration must not exceed the characteristic HCl vibrational deactivation time.

(2) Discharge cooling to approximately 200°K, is necessary to realize the advantages and efficiencies associated with anharmonic pumping and partial inversion operation characteristic of these diatomic media.

(3) The effects of dissociative attachment and fast vibrational self relaxation in HCl do not appear to be a hindrance to laser action.

Furthermore the results of the experiments described herein indicate that:

(4) The requirements for high electron number density and low Townsend parameter (E/n), require the utilization of an auxiliary source of ionization for discharge control.

(5) The HCl doped discharges considered appear to be recombination limited (i.e. $n_e \sim$ [illegible]), although more work is necessary on this matter. The po[illegible]l electron beam current density level required to fulfill the [illegible]ement noted in (1) above is in excess of $1 A/cm^2$ for a 10 μsec excitation pulse.

Recommendations for Further Studies

Based upon these conclusions a redesign of the present experimental apparatus is indicated. In the present system, the post-foil primary electron current density incident on the foil in excess of $20 A/cm^2$. This level would result in foil melting in the present system. The use of a short discharge path is recommended to ameliorate the effects of beam scattering. Shortening of the discharge path would require the use of a large area electron gun, and possibly demand increase of the discharge pressure to utilize the electron beam effeciently. In the present tests the excitation pulse length was much less than the VT relaxation time. Increase of the excitation pulse length will decrease the beam current density required and is highly desirable if $n_e \sim J_b^{\frac{1}{2}}$ scaling remains valid at lower n_e.

Further work on the HCl electric discharge is recommended even though it is realized that the system will require the use of high current electron beams operating close to foil melting limits. Of course electron gun systems also require high voltage power supplies and radiation shielding. Indeed, a

better system may utilize other sources of ionizing radiation (e.g. photoionization), however too little is known of possible interfering processes to recommend these systems as the next step.

VI. ACKNOWLEDGMENT

The authors wish to acknowledge the cooperation and assistance of the Plasmadynamics Group at UARL headed by Robert Bullis. In particular, the participation of William Nighan in the analysis of electron transport data and the deduction of cross sections compatible with these data has proved invaluable. Thomas Churchill, also of the Plasmadynamics Group, has kindly assisted in extending the operating limits of the UARL electron gun for these studies and has lent valuable equipment required for the experiments.

Finally the cooperation of the Systems, Science and Software Hayward Division in designing, building and de-bugging the HV pulser used in these studies is acknowledged.

REFERENCES

1. Shirley, J. A., W. L. Nighan, T. L. Churchill and B. R. Bronfin, "E-Beam HCl Laser," UARL Proposal PL16-1, January 1972.

2. Shirley, J. A., T. L. Churchill and B. R. Bronfin, "E-Beam HCl Laser," UARL Report M911340-6, May 1973.

3. Ziesel, J. P. and G. J. Schulz, "Negative Ion Formation and Vibrational Excitation in Hydrogen Halides", Unpublished data, October 1973.

4. Center, R. E., AVCO Everett Research Laboratories, private communications, April 1973.

5. Nelson L. Y., S. R. Byron, and G. J. Mullaney, Appl. Phys. Lett., 23, 565 (1973).

6. Shirley, J. A., W. L. Nighan, T. L. Churchill and B. R. Bronfin, "E-Beam HCl Laser", UARL Report L911340-4, November 1972.

7. Bailey, V. A. and W. E. Duncanson, Phil Mag., 10, 145 (1930).

8. Nighan, W. L., Phys. Rev. A, 2, 1989 (1970).

9. Frost, L. S. and A. V. Phelps, Phys. Rev., 129, 1621 (1962).

10. Schulz, G. J., Phys. Rev., 125, 229 (1962); ibid, 135, A988 (1964).

11. Christophorou, L. G., R. N. Compton and H. W. Dickson, J. Chem. Phys., 48, 1949 (1968).

12. D. Arnoldi and J. Wolfrum, Chem. Phys. Lett., 9 457, (1971).

13. B. A. Ridley and I. W. M. Smith, Chem. Phys. Lett 9, 457 (1971).

14. Y. Noter, I. Burak, and A. Szoke, J. Chem. Phys., 59, 970 (1973).

15. B. Hopkins and H. L. Chen, J. Chem. Phys., 57, 3816 (1972).

16. S. R. Leone and C. B. Moore, Chem. Phys. Lett., 19, 340 (1973).

17. R. D. Sharma and C. A. Brarr, J. Chem. Phys., 50, 924 (1969).

18. R. D. Sharma and H. Schlossberg, Chem. Phys. Lett., 20, 5 (1973).

19. V. I. Gorshkov, et al., Appl. Opt., 10, 1781 (1971).

20. P. F. Zittel and C. B. Morre, J. Chem. Phys., 59, 6636 (1973).

21. B. Hopkins, H. L. Chem, and R. D. Sharma, J. Chem. Phys., 59, 5788 (1973).

22. N. C. Craig and C. B. Moore, J. Phys. Chem., 75, 1622, (1971).

23. R. V. Ambartzunian, et al., Chem. Phys. Lett., 13, 49 (1972).

24. J. A. Shirley, R. J. Hall and B. R. Bronfin, "E-Beam HCl Laser," UARL Report M911340-9, November, 1973.

25. K. B. Persson, J. Appl. Phys. 36, 3086 (1965).

26. U. Fano, Phys. Rev., 70, 44 (1946).

27. B. N. Subba Rao, Nucl. Instrum. Methods 44, 155 (1966).

28. A. C. Eckbreth and J. W. Davis, "Investigation of Electron-Beam Ionization Control in a Continuous CO_2 Laser Discharge" UARL Report M910990-28, Naval Ordnance Systems Command (N60921-70-C-0219).

29. K. P. Novikova, "The Electron-Ion Recombination Coefficient Measurements in the Stable Argon Plasma" Tenth Int'l Conf. on Phenom. in Ionized Gases (Oxford, Eng.; Sept. 1971). also: J. N. Fox and R. M. Hobson, Phys. Rev. Letters 17, 161 (1966).

30. R. L. Fitzwilson and L. M. Chanin, J. Appl. Phys 44, 5337 (1973).